Atmospheric
Chemistry
and Physics
Discussions

Sources of Surface O_3 in the UK: Tagging O_3 within WRF-Chem

Johana Romero-Alvarez[1,a,b,c], Aurelia Lupaşcu[2], Douglas Lowe[3], Alba Badia[1,4], Scott Acher-Nicholls[5], Steve Dorling[1], Claire E. Reeves[1], Tim Butler[2,6]

[1] School of Environmental Sciences, University of East Anglia, Norwich, UK

5   [2] Institute for Advanced Sustainability Studies (IASS), Potsdam, Germany

[3] Centre for Atmospheric Sciences, School of Earth, Atmospheric and Environmental Sciences, University of Manchester, Manchester, UK

[4] Institute of Environmental Science and Technology (ICTA), Universitat Autònoma de Barcelona, Barcelona, Spain

[5] Centre for Atmospheric Science, Department of Chemistry, University of Cambridge, Cambridge, UK

10   [6] Freie Universität Berlin, Institut für Meteorologie, Berlin, Germany

[a] Now at: Department of Chemistry, University of Colorado Boulder, Boulder, USA

[b] Now at: Cooperative Institute for Research in Environmental Sciences (CIRES), University of Colorado Boulder, Boulder, CO, USA

[c] Now at: NOAA Global Systems Laboratory (GSL), Boulder, CO, USA

15   *Correspondence to*: Johana Romero Alvarez (lero1992@colorado.edu)

Abstract. Tropospheric ozone (O_3) concentrations are known to depend on a combination of hemispheric, regional and local-scale processes. Estimates of how much O_3 is produced locally vs. transported from further afield are essential in air quality management and regulatory policies. Here, a tagged-ozone mechanism within the WRF-Chem model is used to quantify the contributions to surface O_3 in the UK from anthropogenic nitrogen oxide (NOx) emissions from inside and outside the UK
20   during May-August 2015. The contribution of the different source regions to three regulatory O_3 metrics is also examined. It is shown that model simulations predict the concentration and spatial distribution of domain-wide surface O_3 with a mean bias of -3.7 ppbv. Anthropogenic NOx emissions from the UK and Europe account respectively for 13% and 16% of the monthly mean surface O_3 in the UK, as the majority (71%) of O_3 comes from the hemispheric background. The north and the west of the UK experience the largest contributions from hemispheric O_3 with peaks in May, whereas European and UK contributions
25   are most significant in the east and south-east, intensifying towards June and July. It is demonstrated that more stringent emission controls over continental Europe, particularly in western Europe, would be necessary to improve health-related metrics, such as MDA8 O_3 above 50 and 60 ppbv. Emission controls over larger areas, e.g., northern hemisphere, are instead required to lessen the impacts on ecosystems as quantified by metrics such as the AOT40.

30 **1   Introduction**

Tropospheric ozone (O_3) is a pollutant of concern for policy-makers because of its detrimental effects on human health, agriculture and ecosystems (Fuhrer, 2009; WHO, 2016). Near ground level, O_3 has a typical atmospheric lifetime of a few hours. In the free troposphere, however, the lifetime can be up to several weeks (Stevenson et al., 2006). O_3 can therefore be transported from its point of production downwind over long distances crossing countries and continents (Wild et al., 2004;

35 HTAP, 2007). Concentration of O_3 at a given location is therefore dictated by a combination of hemispheric, regional and local-scale factors (Jenkin, 2008). Examples of this are long-range transport of O_3 and its precursors, including stratospheric intrusions, and photochemical reactions happening on a local and regional scale (e.g., Monks, 2000; HTAP, 2007).

Production of O_3 in the troposphere is highly non-linear and depends on the abundance of its precursors, nitrogen oxides (nitrogen dioxide (NO_2) + nitric oxide (NO) = NOx) and volatile organic compounds (VOCs) (Sillman, 1999; Atkinson, 2000).

40 Net production is achieved when NOx is available at moderate levels in a narrow concentration window (Atkinson, 2000; Monks, 2005). Very low concentrations of NOx lead to overall O_3 destruction while high NOx concentrations reduce the O_3 production rate, unless VOCs concentrations rise to balance the competing reactions (Monks, 2005). Furthermore, O_3 concentrations also depend on its deposition and meteorological variables such as temperature, winds (direction and speed), solar radiation intensity and precipitation (e.g., Sillman, 1999; Coyle et al., 2002). For instance, high O_3 concentration episodes

45 in the UK have been associated with heatwave periods (Finch and Palmer, 2020). The contribution of each process varies with location. Remote sites are largely controlled by hemispheric background O_3 (AQEG, 2009). Photochemical pollution episodes, on the other hand, are more severe in the south and east of the UK and O_3 titration by NOx is higher in urban areas (Jenkin, 2008).

In the UK, tighter European precursor emissions controls in the last 30 years have led to a substantial decrease in the

50 concentration of O_3 primary precursors and successfully reduced the severity of the high O_3 concentration episodes (AQEG, 2009; Derwent et al., 2018; Finch and Palmer, 2020). Even so, exposure to surface O_3 continues to cause considerable damage to human health in Europe and the UK leading to an estimated 17,000 premature deaths in 2015 (EEA, 2017). Evidence suggests that annual mean O_3 concentrations in the UK have been increasing in urban/suburban areas and to a lesser extent in rural areas (Jenkin, 2008; AQEG, 2009; Munir et al., 2013; Finch and Palmer, 2020). Reductions in NOx emissions, mainly

55 by road traffic, have led to reductions in the O_3 scavenging in urban areas so that O_3 concentrations have generally increased (Finch and Palmer, 2020). The increase in rural areas, on the other hand, is largely driven by reductions in European regional NOx emissions (Derwent et al., 2018) and rising hemispheric O_3 levels, up to +0.31 ppbv a year over the 20-year 1987–2007 period (Derwent et al., 2007) and +0.25 ppb a year over the 25-year period (Derwent et al., 2013). Accordingly, increasing emissions of precursors in Asia are known to influence O_3 concentrations entering Europe (HTAP, 2010). Therefore, efficient

60 emissions control policies aimed at reducing O_3 concentration in a given region require a holistic assessment of both O_3 transport from outside the region and in-situ O_3 production. Such quantitative estimations can be made by applying source-receptor methods (S-R) within Chemical Transport Models (CTMs).

S-R studies often compare model simulations that include all anthropogenic emissions with those obtained after modifying emissions from a region of interest (the so-called perturbation approach). As O_3 chemistry is non-linear, this approach can lead to unrealistic attribution estimates, e.g., Emmons et al. (2012) underestimated the O_3 contribution by up to a factor of 4 when perturbing NO emissions by 20%. So-called tagged-ozone methods, which use additional diagnostics to follow the reaction of different emissions to the formation of O_3, are better suited to investigate the contribution of different precursors to the total amount of O_3 (Emmons et al., 2012; Grewe et al., 2012; Butler et al., 2018).

Several studies have investigated the contribution of intercontinental transport to O_3 in Europe, in particular from North America and Asia, using different modelling techniques (e.g., Li, 2002; Derwent et al., 2004; Auvray and Bey, 2005; Sudo and Akimoto, 2007; Derwent et al., 2008; Emmons et al., 2012; Derwent et al., 2015; Mertens, 2017; Butler et al., 2018; Lupaşcu and Butler, 2019; Butler et al., 2020). However, these studies do not provide a quantitative estimate of the contribution of the different source regions to the total amount of O_3 over the UK at a regional scale, but rather an estimate at a national scale or at individual locations across Europe or for the European region as a whole.

This paper uses a tagged-ozone mechanism within the WRF-Chem model to quantify contributions to surface O_3 in 12 receptor regions in the UK from anthropogenic NOx emissions from inside and outside the UK. Dividing the UK into several regions serves to separate meteorological features and chemical environments that are known to impact the spatial distribution and temporal variation of air pollutants such as O_3 (Coyle et al., 2002; Jenkin, 2008). We focus on summer 2015, considered as the second warmest year in a row in Europe (WHO, 2016), which saw several heat waves causing elevated O_3 concentrations in Central and Western Europe that exceeded the EU information threshold of 1 hour (h) average mixing ratio of 180 µg m-3 (~90 ppbv) (Tarrasoet al., 2016). We also look at the impact of O_3 on human exposure, crops, and vegetation using two well-known O_3 metrics, the MDA8 and the AOT40. The MDA8 is a health-related metric commonly used to assess the impacts of O_3 exposure on the population (e.g., Reidmiller et al., 2009; Stock et al., 2013; Mar et al., 2016). The metric is defined as the maximum daily 8 h average (MDA8) O_3 values (in ppbv) and is strongly influenced by photochemical episodes (AQEG, 2009). The AOT40 (accumulated ozone above a threshold of 40 ppbv) is commonly used to assess the effects of O_3 on crops and vegetation and is based on exposure over 40 ppbv using only the 1h values measured during daylight hours (between 08:00 and 20:00) Central European Time (CET) over a typical three-month growing season May-July (AQEG, 2009).

Details on the WRF-Chem settings including an introduction to the tagging approach is presented in section 2. Model evaluation is discussed in the Supplemental material. Results for the contributions of UK and European precursor emissions, along with transport across the lateral model boundaries to surface O_3 in the UK are presented and discussed in section 3. Section 4 summarizes our findings.

2 Methods

We used the Weather Research and Forecasting model (WRF) version 3.7.1 (Powers et al., 2017) coupled with chemistry (WRF-Chem) (G. a. Grell et al., 2005). The model domain was centred at 3° E and 53° N, covering most of Europe, as shown in Fig. 1a. The spatial resolution was set to 27 km × 27 km, with 35 vertical levels starting from the surface up to 10 hPa.

The initial and boundary conditions (IC and BC, respectively) for meteorology were obtained from the ERA-Interim reanalysis dataset (Dee et al., 2011), which has a spatial grid resolution of $0.75° \times 0.75°$ and 6-hour temporal resolution. IC and BC for the chemistry fields were extracted from global simulations produced by the Chemistry Transport Model for O_3 and Related Chemical Tracers MOZART-4 GEOS-5 (Emmons et al., 2010), and fed to the model every 3 hours. The schemes used to

100 parameterize the atmospheric processes are listed in Table 1. These are the same schemes deployed in (Mar et al., 2016) to evaluate meteorology, O_3, and NOx fields in a European domain using the MOZART chemical mechanism.

Simulations were conducted for the period between April 24 and August 31 of 2015 for gas-phase chemistry using a tagged-ozone mechanism based on the MOZART-4 chemical scheme. The first week of output was treated as model spin-up and hence discarded. The meteorology was not nudged but re-started every three days as in the methodology adopted in the second

105 phase of the Air Quality Model Evaluation International initiative (AQMEII) (e.g., Im et al., 2014). This decision was made after a test analysis showed that nudging of winds above the planetary boundary layer (PBL) and temperature at all layers, as done in Mar et al. (2016), leads to a representation of hourly NO_2 and O_3 mixing ratios in south East UK that is inconsistent with observations.

Anthropogenic emissions of carbon monoxide (CO), NOx, sulphur dioxide (SO_2) and total non-methane VOCs (NMVOCs)

110 for the European domain, including shipping lines, were taken from the TNO-MACC-III European inventory (Kuenen et al., 2014) for the year 2011. The emissions were provided as yearly totals (kg yr^{-1}) by source sector following the SNAP (selected nomenclature for sources of air pollution) convention at a $0.125° \times 0.0625°$ longitude-latitude resolution. For the UK domain, emissions were taken from the UK national emissions inventory (NAEI) for the year 2014, http://naei.beis.gov.uk/, which has a spatial resolution of 1 km $\times$ 1 km. Biogenic emissions were calculated online using the Model of Emissions of Gases and

115 Aerosols from Nature (MEGAN) version V2.04 (Guenther et al., 2012).

2.1 O_3 tagging mechanism

The contribution of hemispheric O_3 and domestic and European anthropogenic emissions to tropospheric O_3 in the UK is studied using a source attribution technique known as "ozone tagging" in which O_3 molecules are labelled according to the identity of their source regions. This is achieved by tagging NOx emissions at selected source regions. The tagged NOx is

120 tracked through all of the odd nitrogen species (e.g., peroxyacetyl nitrate (PAN), nitric acid (HNO_3) and organic nitrates) to account for the recycling of NOx, and through the formation of O_3. The base chemical mechanism (Model for OZone And Related chemical Tracers MOZART-4) was expanded with additional tracers representing the tagged species for each emission region enabling the direct attribution of O_3 concentrations in receptor regions to specific source regions.

O_3 formation requires both NOx and peroxy radicals from VOCs. There are several tagging methods in existence which can

125 take different approaches to estimate the attribution of O_3 to these two chemically distinct precursors. Butler et al. (2018) provides a summary of the different approaches. The method used here is based on Lupaşcu and Butler (2019), who performed an attribution of O_3 exclusively to NOx precursors, as in Emmons et al. (2012). Butler et al. (2020) has shown that anthropogenic emissions of NMVOC play only a small role in regional scale O_3 production, with the VOC precursors most

important for O_3 production being methane and biogenic NMVOC. As this study is primarily focused on the anthropogenic

130 influence on O_3, the use of NOx tagging for O_3 source attribution is considered appropriate.

2.2 Receptors and source regions

Table 2 lists the tagged sources also highlighted in Fig. 1a and b, respectively. The chemical lateral boundary is defined as an independent source region (LB) and is provided by the MOZART-4 model. Note that the LB tagged-region also includes O_3 contributions of stratospheric origin. Moreover, all O_3 that enters the model domain through the lateral boundaries is tagged

135 as LB, and any tagged O_3 molecule formed within the model domain that exits and re-enters the domain will no longer be attributed to its initial source but instead to the LB.

To generate the receptor regions, the UK domain is divided into its 12 administrative regions as used in previous air quality studies such as Heal et al. (2013), as shown in Fig. 1b: East Anglia, South-East, London area, South-West, Wales, West Midlands, East Midlands, Yorkshire and Humberside, North-East, North-West, Northern Ireland and Scotland.

140 The UK is well known for the regional variability of its weather. Generally, places in the east and south tend to be drier, warmer, sunnier, and less windy than those in the west and north (Jenkin, 2008). Thus, dividing the UK into several regions also serves to separate relevant meteorological features such as temperature, sunshine, precipitation, and wind, as well as emissions within each region that are known to have an impact on the spatial distribution and temporal variation of air pollutants such as O_3 (Coyle et al., 2002; Jenkin, 2008).

145 ## 2.3 O_3 metrics for source contribution assessment

Current European and National air quality standards to mitigate the effects of O_3 on human health are expressed as 8-hour (h) averages. The regulatory framework stablished that the maximum 8 h mean O_3 concentration (MDA8) should not exceeds 120 ug m^{-3} (~60 ppbv) in the European Union (EU), and 100 ug m^{-3} (~50 ppbv) in the UK. Here, the contributions to these health metrics are estimated by computing an 8 h moving mean of O_3 for each receptor region and selecting the days when the MDA8

150 exceeds 50 and 60 ppbv between May to August 2015. Once these were identified, tagged O_3 concentrations were extracted for the same periods, and used in the analysis. The contribution of concentration of tagged O_3 to the cumulative metric AOT40, on the other hand, was calculated by selecting the hours when O_3 mixing ratios exceeded the hourly 40 ppbv thresholds between 08:00 and 20:00 central European time (CET) from May-July over the most relevant arable farming areas in the UK, East Anglia and the South East, see Eq. (1). The target value in the EU and UK is 9000 ppb h^{-1} (~18000 μg m-3 hours) over a

155 typical three- month growing season (May-July) averaged over 5 years.

$$AOT40= \sum_{i=l}^{90d} \max (O_3 - 40) , \tag{1}$$

Once these are identified, tagged O_3 concentrations are extracted for the same period, and used in the analysis.

2.4 Model evaluation

160 Observational data were taken from the UK's Met Office Integrated Data Archive System and the European Monitoring and Evaluation Programme (EMEP). The EMEP air quality monitoring network records hourly measurements at regional background sites, mostly in farmland and rural areas (Tørseth et al., 2012). The choice to only analyze background representative stations is based on the need to provide an evaluation with spatial scales consistent with the model resolution. Kuik et al. (2016), for example, has shown that a 15 km resolution is too coarse to resolve the differences between urban and
165 rural atmospheric chemical composition. The resolution of the domain considered here is even coarser. The EMEP network was therefore selected as it provides surface measurements at sites intended to represent regional background pollution.

Results of the model evaluation are presented in the Supplementary Material. Overall, the model captures the concentrations of O_3 in the European domain well, particularly the spatial distribution in surface O_3. Nonetheless, it tends to underestimate concentrations in most of the assessed sites (mean bias (MB)= -3.71 and correlation coefficient r = 0.65), which is consistent
170 with results from previous modelling studies using the MOZART-4 chemical mechanism over Europe (e.g., Mar et al., 2016).

3 Results and discussion

3.1 Contributions from tagged sources: spatial distribution and temporal variation

Consistent with previous work (e.g, Karamchandani et al., 2017; Lupaşcu and Butler, 2019; Butler et al., 2020), the hemispheric O_3 level, represented here by the LB source region, dominated the monthly O_3 concentrations in the UK during
175 the entire study period with a mean relative contribution of ~71%, exhibiting a maximum in May (mean 76%), a minimum in June (mean 66%), and an increase in August (mean 72%); see Fig. 2. The mean contribution from the Eu super-region (FRA, GER, NET, LUX, BEL, NOS, Rest_CEU and Rest_Eu) accounts for nearly 16 % of the simulated monthly mean O_3. The largest Eu super-region contributions are observed in the UK locations closer to the continental Europe (East Anglia, South-East England and Yorkshire). The smallest Eu super-region contributions are observed over Scotland (May and June) and
180 Ireland (July and August). Emissions from UK sources, on the other hand, accounted for about 13 % of the simulated monthly O_3. The domestic contributions tend to increase in June and decrease again in August. This monthly variation in the O_3 contributions is mainly caused by larger photochemical activity taking place during the summer months (e.g., Monks, 2005). Under these conditions, O_3 is formed by reactions involving the oxidation of NMVOCs in the presence of NOx and under the influence of solar radiation.

185 The spatial distribution of the monthly O_3 concentrations and the absolute contribution of the source regions (UK, LB and Eu super-region) to surface O_3 in the UK are shown in Fig. 3. The first column shows that the monthly surface O_3 concentrations are higher in May than during the summer months, in particular over Ireland, most of the Atlantic Ocean, north of UK, Scandinavia, and the northern North Sea. This is consistent with the Northern Hemisphere mid-latitude spring maximum (Monks, 2000), which is characteristic of remote locations and attributed to both transport of O_3 from the stratosphere to the
190 troposphere (Monks, 2000) and transport of O_3 produced from anthropogenically emitted precursors (NOx and VOCs) (Monks,

2000; Butler et al., 2018). By contrast, the south east of the UK and southern North Sea and continental Europe exhibit sustained high O_3 mixing ratios throughout the entire analyzed period (May to August) reflecting a spring–summer maximum that is frequently attributed to photochemical O_3 production (Monks, 2000).

A marked latitudinal gradient is observed in the monthly O_3 mixing ratios, and in particular during June, July and August.
195 Over the ocean areas, O_3 concentrations tend to be higher at the lower latitudes and in the North Sea, see Figs. 3e, 3i and 3m. Mean O_3 mixing ratios as low as 22 ppbv (Fig. 3i) are observed in most of the UK and Scandinavia in July while mixing ratios as high as 32 ppbv (Fig. 3e) are calculated for southern locations in the UK and Western Europe in June. This is consistent with previous estimates such as those in Butler et al. (2018). Part of the latitudinal gradient in surface O_3 over land can be attributed to the changing O_3 mixing ratios arriving from the Atlantic Ocean. Moreover, high mixing ratios in the south-east
200 UK during summertime are generally associated with photochemical production of O_3 (Monks et al., 2015), in particular from anthropogenic NOx and biogenic NMVOCs emissions (Atkinson, 2000; Butler et al., 2018) as well as transport from of O_3 rich air masses from continental Europe during anticyclonic conditions (Jenkin et al., 2002; Lee et al., 2006; Francis et al., 2011; Romero-Alvarez et al., 2022). Low mean O_3 mixing ratios (as low as 20 ppbv), on the other hand, are observed in the vicinity of the main urban centres e.g., Greater Manchester, the Midlands and the London area (First column Fig. 3). This is
205 because strong titration by excessive local NOx emissions takes place over the main urban centres, whereas high O_3 production rates are expected in the outskirts following the progressive reduction in NOx concentration relative to that of NMVOCs (Jenkin, 2008). Note that the latitudinal gradient across the UK is not evident in high altitude areas in Wales and northern England, having relatively high concentrations of O_3. This is because high altitude areas are much of the time above the shallow boundary layers that form over the lower lying land experiencing larger exposure to O_3.
210 A suitable way to identify the areas influenced by fresh NOx emissions is comparing the mixing ratios of O_3 and Ox (= O_3 + NO_2). Ox is considered a conservative quantity as it is, to a large extent, free from the titration effect of $NO+O_3 \rightarrow NO_2$ (Kley et al., 1994). The effect of titration for July is evident in Fig. 4. When Ox is considered, the concentrations tend to increase over main urban centres such as London, Birmingham, Nottingham, Sheffield, and Greater Manchester, and to a lesser extent over Edinburgh and Glasgow. The NO titration effect is also observed within the main urban centres in continental Europe
215 and along the shipping lanes over the North Sea and the English Channel due to the high NO content of ship emissions compared with that from NMVOCs (Aulinger et al., 2016).

The decrease in the monthly average O_3 mixing ratios towards the summer months over the Atlantic Ocean and most of the British Isles coincides with a progressive reduction in the contribution from LB O_3 over the same areas (second column in Fig. 3). Over remote marine areas, it is likely that the decrease in total O_3 is due to an increase in the photochemical activity and
220 concentration of water vapor during the summer months. O_3 concentrations over land, on the other hand, are likely to be altered by both the changing background contribution from over the ocean, and by processes occurring at the regional and local scale (Jenkin, 2008). Such processes include O_3 scavenging near emission sources, changes in meteorology (wind direction influencing transport, and temperature and radiation influencing photochemical production of O_3), and planetary boundary layer stability (influencing vertical mixing and deposition) (AQEG, 2009). Furthermore, LB O_3 is chemically lost near

225 emissions sources, e.g., the Midlands and London area, shipping lines and over an extended area on the southern part of the Atlantic Ocean, as shown in the map of net midday (11:00–14:00 UTC) near surface LB O_3 chemical production rate in Fig. 5. The figure also shows how the absolute contribution from the LB decreases southward and eastwards. Over the Atlantic, part of this can be attributed to a greater chemical O_3 sink due to the increase in photolysis of O_3 and subsequent production of OH radicals from water vapor (Johnson et al., 1999). Transport of O_3 from the stratosphere might also influence the spatial

230 gradient in the contributions. A marked reduction of LB O_3 is observed over the UK (e.g., a decrease of ~ 10 ppb between LB O_3 over the ocean to over the UK). Depletion of surface O_3 by dry deposition, and chemical loss processes within the UK, such as the reaction of O_3 with NO, may help explain the observed spatial gradient. Reductions in LB O_3 due to the effect of local O_3 scavenging by reaction with NO is illustrated in in Fig. 6, which shows O_X to be fairly spatially homogenous over the UK in July 2015, as an example, with higher mixing ratios of NO_2 in the urban centres.

235   Whereas the absolute contribution from the LB over the UK tends to decline with distance towards the south-east, the absolute contribution of UK anthropogenic NOx emissions to the mean surface O_3 over the UK (Fig. 3 third column) decreases from the south-east to the north and west. The contribution of the UK to UK surface O_3 concentrations is marginal. Over most of the north and the west, the UK contributions ranged from 1–3 ppb. By contrast, maximum UK contributions can reach up to 7 ppb in the east and the Midlands during the summer months. These areas tend to be drier, warmer, and sunnier than those

240 regions further west and north features that are conducive to photochemical O_3 formation (e.g., Coyle et al., 2002; Jenkin, 2008). Furthermore, these regions contain some of the UK largest cities (e.g., London, Birmingham, Nottingham, Manchester and Leeds) which can lead to net O_3 formation downwind of the emission sources where the NOx titration effect is reduced. Indeed, overall, the south and east of the UK exhibit the highest midday (11:00–14:00) O_3 chemical production from UK anthropogenic sources, especially during June and July. Lower O_3 chemical production is instead observed in the west and the

245 north beyond Yorkshire and Humberside, see Fig. 7. On the other hand, the UK makes a positive contribution to O_3 downwind over continental Europe of around 4-8 ppb.

The contribution from European NOx emissions to the mean surface O_3 over the UK (Fig. 3 fourth column) is comparable to that observed from the UK contribution and tends to be higher along much of the eastern, southern and south-west borders, reaching up to 10 ppb in East Anglia during July. This reflects the effective transport of continental O_3 by south-easterly winds

250 during high O_3 pollution events. The European contributions then decrease towards the northern and western areas of the UK, with a minimum (1–3 ppb) over Scotland and Ireland.

Fig. 8 demonstrates that surface O_3 from anthropogenic sources from the Eu super-region is mainly produced outside the UK. This indicates that the contribution from EU emissions to UK surface O_3 is predominantly due to transport of O_3 rather than its NOy precursors. Also, O_3 from EU sources is chemically lost nearby the largest cities in UK (e.g., London area,

255 Birmingham, Nottingham, Manchester and Leeds) and also in the English Channel and North Sea, as shown in the plot of net midday, surface chemical O_3 production rate for from European anthropogenic NOx emissions in Fig. 8. Chemical production peaked in June and July and is generally concentrated over central Europe and the Baltic Sea. By contrast, chemical loss

happened within the main urban centres, nearby point sources and along the shipping routes around Western Europe, the North Sea and English Channel, e.g., sites previously identified to be influenced by NOx titration.

3.1.1   Regional dependence

The simulated contributions of the different source regions to the UK receptor regions for May are presented in Fig. 9. The figure contains 12 nested pie charts, each one associated with a receptor region in the UK that shows the absolute and relative contributions to O_3 mixing ratios in the UK from all anthropogenic NOx sources, including ship emissions. It is worth noting that the contributions from the Rest_Eu source need to be carefully interpreted since these include emissions from the Republic of Ireland, Iberian Peninsula, Southern EU, South-eastern EU, Eastern EU, Northern EU, and ship emissions from the Atlantic, Baltic Sea and the Mediterranean. The LB is the principal contributor to the simulated mean O_3 in every receptor the. LB contributions peak in May (mean absolute contribution 25 ppbv) reflecting the seasonal cycling in the northern hemispheric background O_3 (e.g., Monks, 2000; AQEG, 2009). Contributions are larger in the regions located in the north and west of the UK (e.g., Scotland (30 ppbv), Northern Ireland (28 ppbv), North-East (27 ppbv), the North-West and Wales (26 ppbv)) which are impacted by hemispheric O_3 background due to their geographical positions and low NOx emissions (AQEG, 2009). The contributions in the South-East, East Anglia and East Midlands can be up to 8 ppbv smaller, see Figs. 9 to 12.

A particular pattern is observed during July and August, see Figs. 11 and 12. Although the relative contributions from the LB in the north-western regions are still larger than in the south-western counterparts, the absolute contributions are slightly higher in the South-West (72%, ~21 ppbv) and Wales (76%, ~21 ppbv) compared with Scotland (76%, ~20 ppbv) and Ireland (79%, ~20 ppbv). The UK contributions (both the absolute and the relative values) are higher in the south-east, east and the Midlands and peak in June and July in every receptor area, providing up to 20% of the surface O_3 in East Anglia, 18% in the London area and East Midlands, and 16% in Yorkshire and Humberside and the South East. These numbers make the UK contribution the second biggest source at these locations.

The Eu super-region is the second largest source region in the northern and western UK, with contributions in summertime reaching up to 10% in Scotland and up to 16% in South-West England and 14% in Wales. This source region still has a large impact on the South-East and East Anglia where the relative contributions increased from 12% in May to up to 16% in July. The contributions from ship emissions in the North Sea and English Channel are significantly lower than those from UK sources and Eu super-region (3-4% of the total contribution in the South and East Anglia in May and up to 6% of the total surface O_3 during the summer months). The impact is also less important in the west than in the east and south of the UK.

As for the relative contributions from the different Eu sub-regions (inner circle in Figs. 9, 10, 11 and 12), these are largely influenced by the geographical situation of the receptors and the predominant wind direction. In every receptor, the principal contributor from the Eu super-region is the Rest_Eu source region, providing between 60-70% of the Eu O_3 in May and up to 83% of the O_3 from Eu during summertime. The relative contributions of the Rest_Eu region is larger in the northern and western locations, in particular during the summer months when there is a marked difference in the distribution of the contributions across the UK regions. The summer months see an increase in the input from France, Germany and the Benelux

Atmospheric
Chemistry
and Physics
Discussions
Open Access

EGU

region, in particular over the receptor regions located in the south and east of the UK (e.g., South East England, East Anglia, the London area and the East Midlands). Depending on the predominance of the wind direction, O_3 from anthropogenic sources within France can impact both the west and the east of the UK. The contribution is greater in the southern UK due to the proximity to the source region. The contributions from the Benelux region and Germany are more significant in the east of the

295   UK due to the proximity with the continent (about 14% and 6% of the Eu super-region in the East Anglia during the summer months comes from these two source regions, respectively).

3.2   Contributions to regulatory O_3 metrics

3.2.1   MDA8 O_3 exceeding 50 ppbv

The mean contribution from each source region for the hours when the MDA8 O_3 exceeded 50 ppbv at each receptor area from

300   May to August is presented in Fig. 13. The figure shows large contributions from source regions that were not seen as dominant sources. France, for example, becomes a major source particularly in receptors located in the south and east of the UK. The absolute mean contributions at the sites sometimes exceed the input from the LB O_3 (mean value ranging between 10 and 15 ppbv, and maximum reaching up to 35 ppbv in the London area). The impact of UK NO_X on O_3 varies across the sites, but in general its share increased from the south-east to the north. In the Midlands, the North East, North West, Scotland and

305   Yorkshire and the Humberside, O_3 from UK sources becomes dominant surpassing the LB mean input in most of the receptor regions. In the remaining locations, the UK source is the third largest input for surface O_3 with the exception of the South West where most of the O_3 comes from France (mean ~18 ppbv), the LB (mean ~14 ppbv), NOS (mean ~6 ppbv) and Rest_Eu (mean ~8 ppbv).

The Rest_Eu region has a larger impact in the southern sites, in particular in East Anglia where the share can be greater than

310   the contributions from domestic sources (mean value ~7 ppbv). The impact decreases towards the northern regions showing sporadic large values e.g., the North West which could be apportioned to emission sources in the Irish Sea.

The impact from the shipping component (NOS) also becomes important in all receptor regions with an estimated mean of 4-7 ppbv. O_3 from Central Eu, Germany, Netherlands, Belgium and Luxembourg, on the other hand, is almost negligible in the west of the UK (mean less than 1 ppbv). However, their impact increases towards the east and north with mean values ranging

315   about 1-6 ppbv (e.g., in the East Midlands, North-East, Yorkshire and the Humberside and Scotland) reflecting the efficient transport of polluted-loaded air masses under anticyclonic conditions.

3.2.2   MDA8 O_3 exceeding 60 ppbv

Fig. 14 shows mean contribution at each receptor area to hourly surface O_3 when the MDA8 O_3 exceeded the 60 ppbv threshold. Note that there were two occasions when the modelled MDA8 exceeds 60 ppb and the main occasion being the episode on the

320   1st July. France is the most significant contributor to the build-up of O_3 when the mixing ratios exceeded the EU threshold in South East England (mean ~18), East Anglia (mean ~21) and the London area (mean ~26 ppbv). O_3 from UK NOx emissions,

on the other hand, has a greater impact on the East Midlands (mean ~16 ppbv), Yorkshire and Humberside (mean ~15 ppbv). In the South-East and the London area, the contributions from Rest_Eu equal those from UK O_3, while the influence is comparable to that from the west and Central Europe in the rest of the regions. As in the contributions to the MDA8 O_3 of 50

325 discussed before, the lateral boundary component remained nearly constant in all receptors areas with a mean contribution about 12 ppbv. The impacts from the North Sea and English Channel are also important in all receptor regions with a similar estimated mean between 4-7 ppbv. Results suggest that ship emissions along these routes affect the air quality of the UK, in particular over the East and South-east. However, the current model configuration does not consider the chemical evolution of the different emitted species (chemical loss and production rates) during the dispersion of the ship plume. In fact, once species

330 are emitted, they are instantaneously mixed in each model grid cells (27 x 27 km). In the case of chemically reactive species such as NOx, this can lead to overestimations of both NOx and O_3 concentrations due to the non-linearity of the chemical processes involving NOx and O_3 evolution during the dispersion of the ship plume (e.g., Huszar et al., 2010; Van Der Werf et al., 2010).

3.2.3   AOT40 index

335 The average simulated AOT40 for 2015 at the two most relevant arable areas in the UK: East Anglia and the South East is 3674 and 1833 µg m-3 hours, respectively (the target value for the EU and UK is (~18000 µg m-3 hours). Fig. 15 shows the source contributions to the surface O_3 when the mixing ratio exceeded 40 ppbv during the daytime hours (08:00 and 20:00) Central European Time from May to July in two receptor regions in the UK. Compared with the contributions to the MDA8 O_3 of 50 and 60 ppbv, when the exceedance to the hourly surface O_3 mixing ratios above 40 ppbv are considered, the LB

340 component becomes the dominant source in both receptor regions as its threshold is close to the tropospheric baseline ozone level (estimated mean concentration between 21-24 ppbv). The second largest contributor is the UK with a higher impact in the East Anglia region (estimated mean concentration 10 ppbv) than in the South East (estimated mean concentration 6 ppbv). The third, fourth and fifth contributions in East Anglia come from the Rest_Eu and Rest_CEU regions and France, while in the South East the contributions come from the North Sea and English Channel, Rest_Eu and Germany. The contributions

345 from the Netherlands, Belgium and Luxembourg become almost negligible.

Note that the AOT40 metric assesses the impacts of O_3 on the vegetation by considering an O_3 threshold (e.g., concentrations above 40 ppbv) during the months when plant growth is most likely to be affected and when daytime O_3 concentrations are at their highest. However, research experiments have shown that the response of plants to O_3 exposure is non-linear due to a mismatch between the peak daytime O_3 concentrations and stomatal opening (Heath et al., 2009). This means that the effective

350 amount of O_3 taken up by plants is not always correlated to the ambient O_3 concentrations. The AOT40 index does not account for the plant's physiological control of stomatal opening, which limits the potential of the index to accurately assess the impacts of O_3 on the vegetation. Future work should consider flux-based metrics which have proven to be more suitable for ozone-risk assessment on plants as they take into account the ambient concentration of O_3, the physiological control on stomatal openings,

and the efficiency of leaf antioxidant system (Fares et al., 2010) as well as improving the O₃ deposition routines in WRF-Chem
355   so that they can take into account factors such as stomatal opening cycles.

4   Conclusions

An O₃ tagging technique within the WRF-Chem model was used to investigate the origin of surface O₃ from May to August
2015 and the contribution of different source regions to O₃ regulatory metrics in the UK. Evaluation against observations
presented in the supplemental material has shown that the model setup gives a good representation of O₃ in the European
360   domain.

Domain wide examination demonstrates that the hemispheric O₃, here represented by lateral boundary O₃, has the largest
impact on the concentrations of O₃ in the UK, with an estimated 71% of the modelled monthly mean surface O₃ coming from
this source region. About 16 % of modelled surface O₃ is produced from anthropogenic NOx emissions within the EU that
contain lumped NOx emissions from continental Europe, the Republic of Ireland and from ship emissions in the Atlantic,
365   North Sea, Baltic Sea and the Mediterranean. UK emissions (England, Scotland, Wales and Northern Ireland) contributed
13%.

Assessment of the contributions to different receptor regions in the UK revealed that the UK relative contribution to UK surface
O₃ tends to be higher in June and July with a marked spatial gradient, with high mixing ratios obtained in the south-east and
lower values in the north and west. In fact, UK NOx emissions are the second largest contributor to surface O₃ in the East
370   Midlands, West Midlands, Yorkshire and the Humberside, East Anglia, South East England and the London area after the
lateral boundary source region. The monthly and spatial variation of the contribution of UK NOx emissions to UK surface O₃
is primarily caused by larger photochemical activity taking place during the summer months in the south and downwind of
emissions sources. Similarly, the absolute contribution from European sources to UK surface O₃ tends to be higher in June and
July and along much of the eastern, southern and south-west borders reflecting the effective transport of continental O₃ by
375   south-easterly winds during O₃ pollution events. The tagging technique also shows that O₃ from this region is generally
transported to the UK rather than produced in-situ.

O₃ tagging has also made it possible to demonstrate that more stringent emission controls would be required in different source
regions for compliance of UK and EU O₃ standards, e.g., MDA8 O₃ of 50 and 60 ppbv. Emissions controls in France, in
particular, would significantly reduce O₃ concentrations in South East, South West and East Anglia while domestic emissions
380   controls are more relevant for the Midlands and the north of the UK. Exposure thresholds, such as those considered in the
AOT40 O₃ metric, are instead most affected by lateral boundary components in first place followed by UK NOx emissions.
Emissions controls in regions such as the East Midlands, West Midlands, Yorkshire and the Humberside, East Anglia, South
East England and the London area will aid in the mitigation of the impacts on crops. Nonetheless, emission controls will be
also necessary over the larger Northern hemisphere area.

385   The results from model simulation should be interpreted in the context of the observed negative and positive bias (up to -15
ppbv and + 5 ppbv, respectively) and the underestimation of the number of days with the MDA8 O₃ above 50 and 60 ppbv and

AOT40 metric. Also, controlling emissions of NO would not necessarily translate into reduction of O_3 concentration in the UK. In fact, For the AOT40 measure in rural regions it seems that reducing UK emissions might well still help improve the situation whereas for urban regions reducing NOx will increase O_3 concentrations due to a reduction in the titration effect. In this regard, future work should consider extending the tagging mechanism to include the competing NOx–VOC interactions in O_3 production. Emission perturbation studies might also complement the investigation by adding an understanding of response of O_3 to different emission control scenarios.

Code and data availability

The WRF-Chem model is publicly available on http://www2. mmm.ucar.edu/wrf/users/download/get_source.html. The modification introduced and described in Section 2 as well as the model data can be provided upon request.

Author contributions

JRA conducted the numerical simulations and analyzed the data. JRA wrote the paper with contribution from all authors.

Competing interests

The authors declare that they have no conflict of interest.

Acknowledgements

References

AQEG (2009). Ozone in the United Kingdom. Report of the UK Air Quality Expert Group, AQEG. Prepared for the Department for Environment, Food and Rural Affairs, the Scottish Executive, the Welsh Assembly and the Department of the Environment in Northern Ireland. *Defra Defra publications, London*. ISBN 978-0-85521-184-4

Atkinson, R. (2000). Atmospheric chemistry of VOCs and NOx. *Atmospheric Environment*, *34*(12–14), 2063–2101. https://doi.org/10.1016/S1352-2310(99)00460-4

Aulinger, A., Matthias, V., Zeretzke, M., Bieser, J., Quante, M., & Backes, A. (2016). The impact of shipping emissions on air pollution in the greater North Sea region - Part 1: Current emissions and concentrations. *Atmospheric Chemistry and Physics*, *16*(2), 739–758. https://doi.org/10.5194/acp-16-739-2016

Beljaars, A. C. M. (1995). The parametrization of surface fluxes in large scale models under free convection. *Quarterly Journal of the Royal Meteorological Society*, *121*(522), 255–270. https://doi.org/10.1002/qj.49712152203

Butler, T., Lupascu, A., Coates, J., & Zhu, S. (2018). TOAST 1.0: Tropospheric ozone attribution of sources with tagging for CESM 1.2.2. *Geoscientific Model Development*, *11*(7), 2825–2840. https://doi.org/10.5194/gmd-11-2825-2018

Butler, T., Lupascu, A., & Nalam, A. (2020). Attribution of ground-level ozone to anthropogenic and natural sources of NO<sub>x</sub> and reactive carbon in a global chemical transport model. *Atmospheric Chemistry and Physics Discussions*, *x*, 1–41. https://doi.org/10.5194/acp-2020-436

Chen, F., & Dudhia, J. (2001). Coupling an Advanced Land Surface–Hydrology Model with the Penn State–NCAR MM5 Modeling System. Part I: Model Implementation and Sensitivity. *Monthly Weather Review*, *129*(4), 569–585. https://doi.org/10.1175/1520-0493(2001)129<0569:CAALSH>2.0.CO;2

Chou, M.-D., & Suarez, M. J. (1994). An efficient thermal infrared radiation parameterization for use in general circulation models. *NASA Tech. Memo*, *104606*(3), 85. http://citeseerx.ist.psu.edu/viewdoc/summary?doi=10.1.1.26.4850

Coyle, M., Smith, R. I., Stedman, J. R., Weston, K. J., & Fowler, D. (2002). Quantifying the spatial distribution of surface ozone concentration in the UK. *Atmospheric Environment*, *36*(6), 1013–1024. https://doi.org/10.1016/S1352-2310(01)00303-X

Dee, D. P., Uppala, S. M., Simmons, A. J., Berrisford, P., Poli, P., Kobayashi, S., Andrae, U., Balmaseda, M. A., Balsamo, G., Bauer, P., Bechtold, P., Beljaars, A. C. M., van de Berg, L., Bidlot, J., Bormann, N., Delsol, C., Dragani, R., Fuentes, M., Geer, A. J., … Vitart, F. (2011). The ERA-Interim reanalysis: Configuration and performance of the data assimilation system. *Quarterly Journal of the Royal Meteorological Society*, *137*(656), 553–597. https://doi.org/10.1002/qj.828

Derwent, R. G., Stevenson, D. S., Collins, W. J., & Johnson, C. E. (2004). Intercontinental transport and the origins of the ozone observed at surface sites in Europe. *Atmospheric Environment*, *38*(13), 1891–1901. https://doi.org/10.1016/j.atmosenv.2004.01.008

Derwent, R. G, Simmonds, P. G., Manning, A. J., & Spain, T. G. (2007). Trends over a 20-year period from 1987 to 2007 in surface ozone at the atmospheric research station, Mace Head, Ireland. *Atmospheric Environment*, *41*(39), 9091–9098.

https://doi.org/10.1016/j.atmosenv.2007.08.008

Derwent, R. G., Manning, A. J., Simmonds, P. G., Spain, T. G., & O'Doherty, S. (2018). Long-term trends in ozone in baseline
and European regionally-polluted air at Mace Head, Ireland over a 30-year period. *Atmospheric Environment*, *179*(February), 279–287. https://doi.org/10.1016/j.atmosenv.2018.02.024

Derwent, R. G, Manning, A. J., Simmonds, P. G., Spain, T. G., & O'Doherty, S. (2013). Analysis and interpretation of 25
years of ozone observations at the Mace Head Atmospheric Research Station on the Atlantic Ocean coast of Ireland from
1987 to 2012. *Atmospheric Environment*, *80*, 361–368. https://doi.org/10.1016/j.atmosenv.2013.08.003

EEA. (2017). *Air quality in Europe — 2017 report* (Issue 13). https://doi.org/10.2800/850018

Emmons, L. K., Hess, P. G., Lamarque, J. F., & Pfister, G. G. (2012). Tagged ozone mechanism for MOZART-4, CAM-chem
and other chemical transport models. *Geosci. Model Dev.*, *5*(6), 1531–1542. https://doi.org/10.5194/gmd-5-1531-2012

Emmons, L. K., Walters, S., Hess, P. G., Lamarque, J. F., Pfister, G. G., Fillmore, D., Granier, C., Guenther, A., Kinnison, D.,
Laepple, T., Orlando, J., Tie, X., Tyndall, G., Wiedinmyer, C., Baughcum, S. L., & Kloster, S. (2010). Description and
evaluation of the Model for Ozone and Related chemical Tracers, version 4 (MOZART-4). *Geoscientific Model
Development*, *3*(1), 43–67. https://doi.org/10.5194/gmd-3-43-2010

Fares, S., Goldstein, A., & Loreto, F. (2010). Determinants of ozone fluxes and metrics for ozone risk assessment in plants.
Journal of Experimental Botany, *61*(3), 629–633. https://doi.org/10.1093/jxb/erp336

Finch, D. P., & Palmer, P. I. (2020). Increasing ambient surface ozone levels over the UK accompanied by fewer extreme
events. *Atmospheric Environment*, *237*(June), 117627. https://doi.org/10.1016/j.atmosenv.2020.117627

Francis, X. V., Chemel, C., Sokhi, R. S., Norton, E. G., Ricketts, H. M. A., & Fisher, B. E. A. (2011). Mechanisms responsible
for the build-up of ozone over South East England during the August 2003 heatwave. *Atmospheric Environment*, *45*(38),
6880–6890. https://doi.org/10.1016/j.atmosenv.2011.04.035

Fuhrer, J. (2009). Ozone risk for crops and pastures in present and future climates. *Naturwissenschaften*, *96*(2), 173–194.
https://doi.org/10.1007/s00114-008-0468-7

Grell, G. A., & Dévényi, D. (2002). A generalized approach to parameterizing convection combining ensemble and data
assimilation techniques. *Geophysical Research Letters*, *29*(14), 10–13. https://doi.org/10.1029/2002GL015311

Grell, G. a., Peckham, S. E., Schmitz, R., McKeen, S. a., Frost, G., Skamarock, W. C., & Eder, B. (2005). Fully coupled
"online" chemistry within the WRF model. *Atmospheric Environment*, *39*(37), 6957–6975.
https://doi.org/10.1016/j.atmosenv.2005.04.027

Grewe, V., Dahlmann, K., Matthes, S., & Steinbrecht, W. (2012). Attributing ozone to NOx emissions: Implications for climate
mitigation measures. *Atmospheric Environment*, *59*(x), 102–107. https://doi.org/10.1016/j.atmosenv.2012.05.002

Guenther, A. B., Jiang, X., Heald, C. L., Sakulyanontvittaya, T., Duhl, T., Emmons, L. K., & Wang, X. (2012). The model of
emissions of gases and aerosols from nature version 2.1 (MEGAN2.1): An extended and updated framework for
modeling biogenic emissions. *Geoscientific Model Development*, *5*(6), 1471–1492. https://doi.org/10.5194/gmd-5-1471

Heal, M. R., Heaviside, C., Doherty, R. M., Vieno, M., Stevenson, D. S., & Vardoulakis, S. (2013). Health burdens of surface

Atmospheric
Chemistry
and Physics
Discussions

ozone in the UK for a range of future scenarios. *Environment International*, *61*, 36–44.
https://doi.org/10.1016/j.envint.2013.09.010

Heath, R. L., Lefohn, A. S., & Musselman, R. C. (2009). Temporal processes that contribute to nonlinearity in vegetation
485   responses to ozone exposure and dose. *Atmospheric Environment*, *43*(18), 2919–2928.
https://doi.org/10.1016/j.atmosenv.2009.03.011

Hong, S.-Y., Noh, Y., & Dudhia, J. (2006). A new vertical diffusion package with an explicit treatment of entrainment
processes. *Monthly Weather Review*, *134*(9), 2318–2341. https://doi.org/10.1175/MWR3199.1

HTAP. (2007). *Hemispheric Transport of Air Pollution 2007* (Issue 17). https://doi.org/10.18356/2c908168-en

490   Huszar, P., Cariolle, D., Paoli, R., Halenka, T., Belda, M., Schlager, H., Miksovsky, J., & Pisoft, P. (2010). Modeling the
regional impact of ship emissions on NOxand ozone levels over the Eastern Atlantic and Western Europe using ship
plume parameterization. *Atmospheric Chemistry and Physics*, *10*(14), 6645–6660. https://doi.org/10.5194/acp-10-6645-
2010

Iacono, M. J., Delamere, J. S., Mlawer, E. J., Shephard, M. W., Clough, S. A., & Collins, W. D. (2008). Radiative forcing by
495   long-lived greenhouse gases: Calculations with the AER radiative transfer models. *Journal of Geophysical Research
Atmospheres*, *113*(13), 1–8. https://doi.org/10.1029/2008JD009944

Im, U., Bianconi, R., Solazzo, E., Kioutsioukis, I., Badia, A., Balzarini, A., Baró, R., Bellasio, R., Brunner, D., Chemel, C.,
Curci, G., Denier van der Gon, H., Flemming, J., Forkel, R., Giordano, L., Jiménez-Guerrero, P., Hirtl, M., Hodzic, A.,
Honzak, L., … Yahya, K. (2014). Evaluation of operational on-line-coupled regional air quality models over Europe and
500   North America in the context of AQMEII phase 2. Part I: Ozone. *Atmospheric Environment*, *115*, 404–420.
https://doi.org/10.1016/j.atmosenv.2014.09.042

Jenkin, M. E. (2008). Trends in ozone concentration distributions in the UK since 1990: Local, regional and global influences.
Atmospheric Environment, *42*(21), 5434–5445. https://doi.org/10.1016/j.atmosenv.2008.02.036

Jenkin, M. E., Davies, T. J., & Stedman, J. R. (2002). The origin and day of week dependence of photochemical ozone episodes
505   in the UK. *Atmospheric Environment*, *36*(6), 999–1012. https://doi.org/10.1016/S1352-2310(01)00360-0

Romero-Alvarez, J., Lowe, D., Archer-Nicholls, S., Bandy, B., Crilley, L., Bloss, W., Reeves, C. The Contributing Processes
to the Build-up of Ozone in South East England During a Heat Wave Period. In preparation for *Atmospheric
Environment*, 2022.

Johnson, C. E., Collins, W. J., Stevenson, D. S., & Derwent, R. G. (1999). Relative roles of climate and emissions changes on
510   future tropospheric oxidant concentrations. *Journal of Geophysical Research Atmospheres*, *104*(D15), 18631–18645.
https://doi.org/10.1029/1999JD900204

Karamchandani, P., Long, Y., Pirovano, G., Balzarini, A., & Yarwood, G. (2017). Source-sector contributions to European
ozone and fine PM in 2010 using AQMEII modeling data. *Atmospheric Chemistry and Physics*, *17*(9), 5643–5664.
https://doi.org/10.5194/acp-17-5643-2017

515 Kley, D., Geiss, H., & Mohnen, V. A. (1994). Tropospheric ozone at elevated sites and precursor emissions in the United

States and Europe. *Atmospheric Environment*, *28*(1), 149–158. https://doi.org/10.1016/1352-2310(94)90030-2

Kuik, F., Lauer, A., Churkina, G., Denier van der Gon, H. A. C., Fenner, D., Mar, K. A., & Butler, T. M. (2016). Air quality modelling in the Berlin-Brandenburg region using WRF-Chem v3.7.1: sensitivity to resolution of model grid and input data. *Geoscientific Model Development Discussions*, *0*(2), 1–46. https://doi.org/10.5194/gmd-2016-190

520 Lee, J. D., Lewis, A. C., Monks, P. S., Jacob, M., Hamilton, J. F., Hopkins, J. R., Watson, N. M., Saxton, J. E., Ennis, C., Carpenter, L. J., Carslaw, N., Fleming, Z., Bandy, B. J., Oram, D. E., Penkett, S. A., Slemr, J., Norton, E., Rickard, A. R., K Whalley, L., … Jenkin, M. E. (2006). Ozone photochemistry and elevated isoprene during the UK heatwave of august 2003. *Atmospheric Environment*, *40*(39), 7598–7613. https://doi.org/10.1016/j.atmosenv.2006.06.057

Lin, Y.-L., Farley, R. D., & Orville, H. D. (1983). Bulk Parameterization of the Snow Field in a Cloud Model. In *Journal of*
525 *Climate and Applied Meteorology* (Vol. 22, Issue 6, pp. 1065–1092). https://doi.org/10.1175/1520-0450(1983)022<1065:BPOTSF>2.0.CO;2

Lupaşcu, A., & Butler, T. (2019). Source attribution of European surface O3 using a tagged O3 mechanism. *Atmospheric Chemistry and Physics Discussions*, *x*, 1–32. https://doi.org/10.5194/acp-2019-225

Mar, K. A., Ojha, N., Pozzer, A., & Butler, T. M. (2016). Ozone air quality simulations with WRF-Chem (v3.5.1) over Europe:
530 Model evaluation and chemical mechanism comparison. *Geoscientific Model Development*, *9*(10), 3699–3728. https://doi.org/10.5194/gmd-9-3699-2016

Mertens, M., Grewe, V., Rieger, V. S., & Jöckel, P. (2018). Revisiting the contribution of land transport and shipping emissions to tropospheric ozone. *Atmospheric Chemistry and Physics*, *18*(8), 5567–5588. https://doi.org/10.5194/acp-18-5567-2018

535 Monks, P. S. (2000). A review of the observations and origins of the spring ozone maximum. *Atmospheric Environment*, *34*(21), 3545–3561. https://doi.org/10.1016/S1352-2310(00)00129-1

Monks, P. S. (2005). Gas-phase radical chemistry in the troposphere. *Chemical Society Reviews*, *34*(5), 376–395. https://doi.org/10.1039/b307982c

Munir, S., Chen, H., & Ropkins, K. (2013). Quantifying temporal trends in ground level ozone concentration in the UK.
540 *Science of the Total Environment*, *458–460*, 217–227. https://doi.org/10.1016/j.scitotenv.2013.04.045

Powers, J. G., Klemp, J. B., Skamarock, W. C., Davis, C. A., Dudhia, J., Gill, D. O., Coen, J. L., Gochis, D. J., Ahmadov, R., Peckham, S. E., Grell, G. A., Michalakes, J., Trahan, S., Benjamin, S. G., Alexander, C. R., Dimego, G. J., Wang, W., Schwartz, C. S., Romine, G. S., … Duda, M. G. (2017). The weather research and forecasting model: Overview, system efforts, and future directions. *Bulletin of the American Meteorological Society*, *98*(8), 1717–1737.
545 https://doi.org/10.1175/BAMS-D-15-00308.1

Reidmiller, D. R., Fiore, A. M., Jaffe, D. A., Bergmann, D., Cuvelier, C., Dentener, F. J., Duncan, B. N., Folberth, G., Gauss, M., Gong, S., Hess, P., Jonson, J. E., Keating, T., Lupu, A., Marmer, E., Park, R., Schultz, M. G., Shindell, D. T., Szopa, S., … Zuber, A. (2009). The influence of foreign vs. North American emissions on surface ozone in the US. *Atmospheric Chemistry and Physics*, *9*(14), 5027–5042. https://doi.org/10.5194/acp-9-5027-2009

17

550   Sillman, S. (1999). The relation between ozone, NO and hydrocarbons. *Atmospheric Environment*, *33*, 1821–1845.

Stevenson, D. S., Dentener, F. J., Schultz, M. G., Ellingsen, K., van Noije, T. P. C., Wild, O., Zeng, G., Amann, M., Atherton, C. S., Bell, N., Bergmann, D. J., Bey, I., Butler, T., Cofala, J., Collins, W. J., Derwent, R. G., Doherty, R. M., Drevet, J., Eskes, H. J., … Szopa, S. (2006). Multimodel ensemble simulations of present-day and near-future tropospheric ozone. *Geophysical Research Letters*, *111*(8). https://doi.org/10.1029/2005JD006338

555   Stock, Z. S., Russo, M. R., Butler, T. M., Archibald, A. T., Lawrence, M. G., Telford, P. J., Abraham, N. L., & Pyle, J. A. (2013). Modelling the impact of megacities on local, regional and global tropospheric ozone and the deposition of nitrogen species. *Atmospheric Chemistry and Physics*, *13*(24), 12215–12231. https://doi.org/10.5194/acp-13-12215-2013

Tarrason, L., Hamer, P., Guerreiro, C., Meleux, F., & Rouil, L. (2016). Interim Annual Assessment Report for 2015 - European
560   air quality in 2015. 10.13140/RG.2.2.15127.78249

Tørseth, K., Aas, W., Breivik, K., Fjeraa, A. M., Fiebig, M., Hjellbrekke, A. G., Lund Myhre, C., Solberg, S., & Yttri, K. E. (2012). Introduction to the European Monitoring and Evaluation Programme (EMEP) and observed atmospheric composition change during 1972-2009. *Atmospheric Chemistry and Physics*, *12*(12), 5447–5481. https://doi.org/10.5194/acp-12-5447-2012

565   Van Der Werf, G. R., Randerson, J. T., Giglio, L., Collatz, G. J., Mu, M., Kasibhatla, P. S., Morton, D. C., Defries, R. S., Jin, Y., & Van Leeuwen, T. T. (2010). Global fire emissions and the contribution of deforestation, savanna, forest, agricultural, and peat fires (1997-2009). *Atmospheric Chemistry and Physics*, *10*(23), 11707–11735. https://doi.org/10.5194/acp-10-11707-2010

WHO. (2016). Ambient Air Pollution: A global assessment of exposure and burden of disease. In *World Health Organization*.
570   https://doi.org/9789241511353

Wild, O., Pochanart, P., & Akimoto, H. (2004). Trans-Eurasian transport of ozone and its precursors. *Journal of Geophysical Research D: Atmospheres*, *109*(11), 1–16. https://doi.org/10.1029/2003JD004501

575

580

Atmospheric
Chemistry
and Physics
Discussions

Table 1. Parameterizations options used in the study

Process	Scheme
Cloud microphysics	Lin et al. scheme (Lin et al., 1983)
Radiation (short wave)	RRTMG (Iacono et al., 2008)
Radiation (long wave)	Goddard shortwave scheme (Chou and Suarez, 1994)
Boundary layer physics	Yonsei University scheme (Hong et al., 2006)
Surface layer	MM5 similarity based on Monin–Obukhov scheme (Beljaars, 1995)
Land surface processes	Noah land surface model (Chen and Dudhia, 2001)
Cumulus convection	Grell 3-D scheme (Grell and Dévényi, 2002)

585

Table 2. List of tagged source regions

Source region	Abbr.	List of countries or source type
Hemispheric O_3	LB	Lateral boundaries
France	FRA	France
Germany	GER	Germany
Netherlands	NET	Netherlands
Luxemburg	LUX	Luxemburg
Belgium	BEL	Belgium
North Sea and English Channel	NOS	North Sea and English Chanel
UK	UK	England, Scotland, Wales and Northern Ireland
Rest of central Europe	Rest_CEU	Austria, Switzerland, the Czech Republic, Hungary, Poland, Slovakia, Slovenia and Romania
Rest of Europe	Rest_Eu	Remaining areas in the model domain including the Republic of Ireland, Iberian Peninsula, Southern Europe, South-eastern Europe, Eastern Europe, Northern Europe, and shipping emissions from the Atlantic, Baltic Sea and the Mediterranean.

590

595

600

19
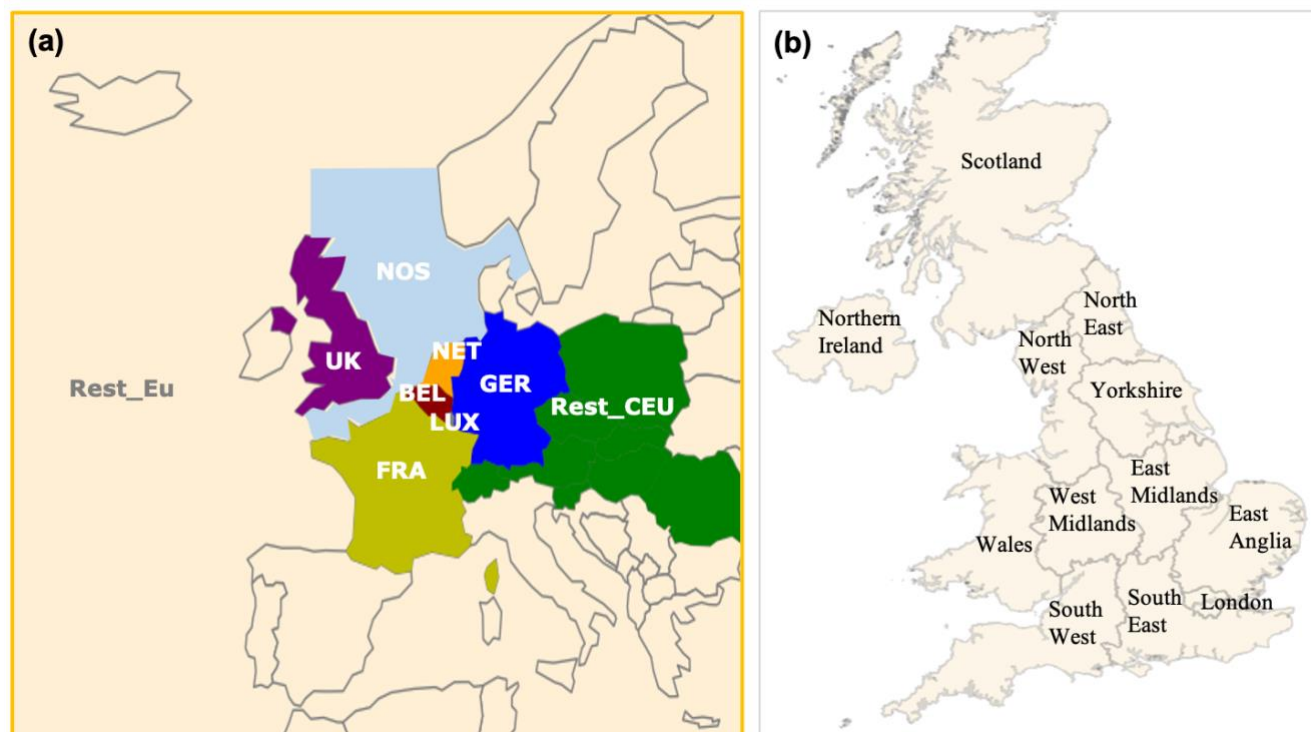
Figure 1. Source regions and receptors: (a) division of domain into 9 source regions. Note that Rest_Eu source region also includes ship emissions from the Atlantic, Mediterranean and Baltic Sea whilst emissions from shipping routes in the North Sea and the English Channel are tagged as NOS. The orange line surrounding the domain indicates LB tag. (b) map of the UK showing the receptor regions.

605

610

615

Atmospheric
Chemistry
and Physics
Discussions

620
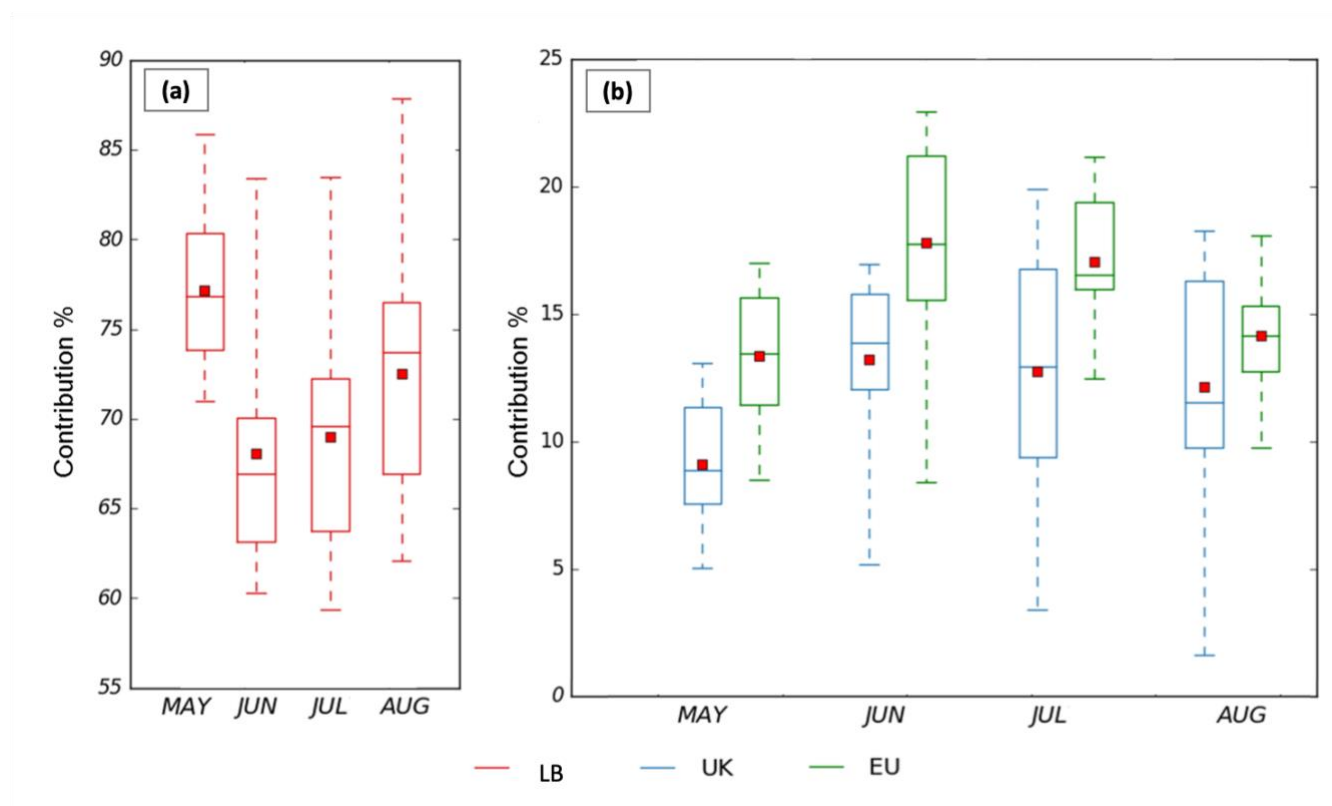
Figure 2. Monthly relative contributions (%) to surface O_3 in the UK from May to August 2015 from (a) the lateral boundaries (LB) and (b) the UK and the Eu super-region. The lower and upper end of the boxes indicate the 25th and 75th percentiles, the central bar the median, and the red square the mean. Whiskers indicate the maximum and minimum. Note the differences in the scale in the y axis.

625

630

635
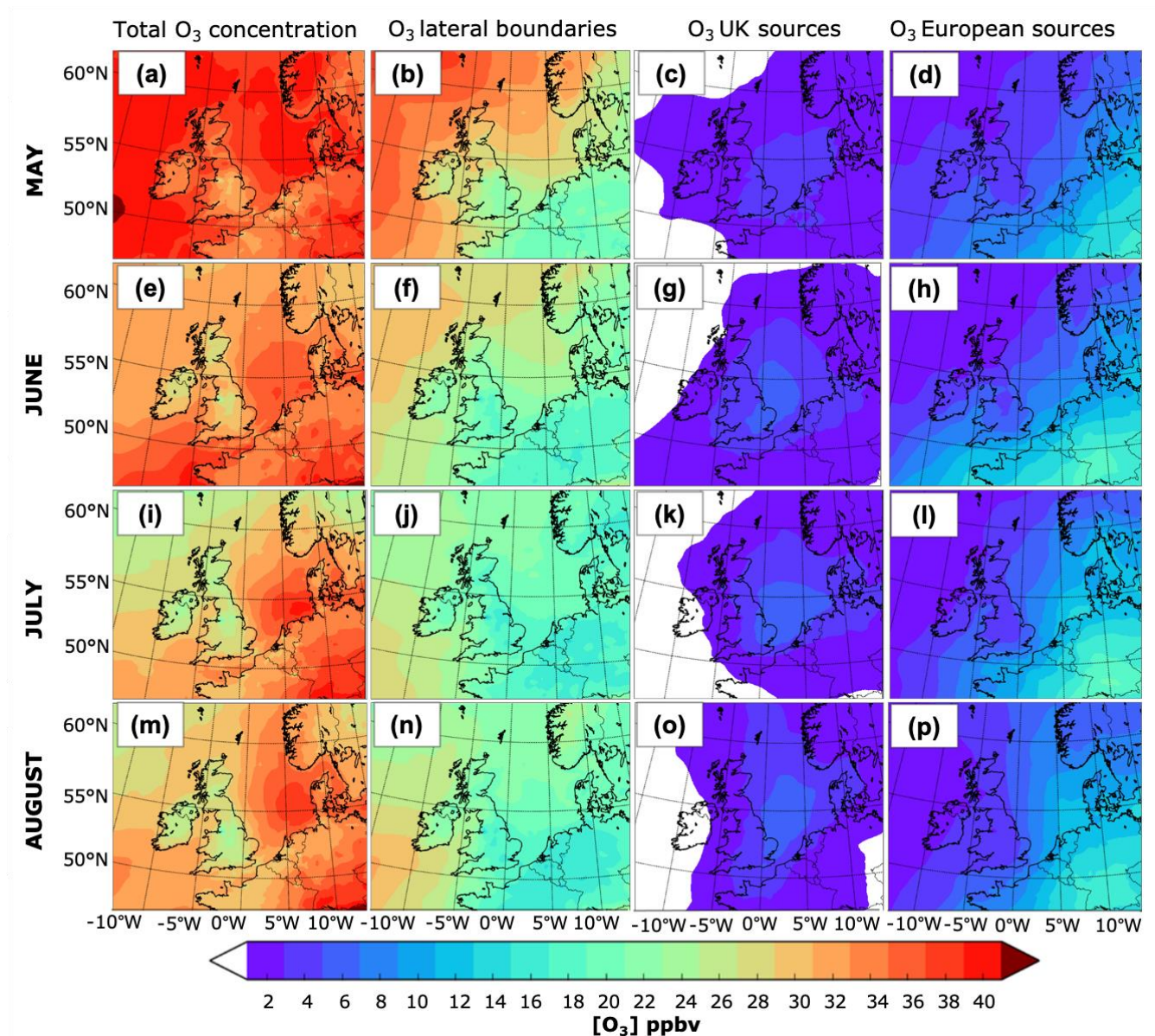
Figure 3. Spatial distribution of the monthly mean surface O$_3$ from May to August 2015. The first column depicts the mean O$_3$ concentration in May, June, July and August; the absolute monthly contribution from the lateral boundaries is shown in the second column; the third column shows the contribution from UK emissions; and the contribution from the Eu super-region, which includes emissions from main shipping routes over the European seas and the Atlantic, is presented in the fourth column.

640
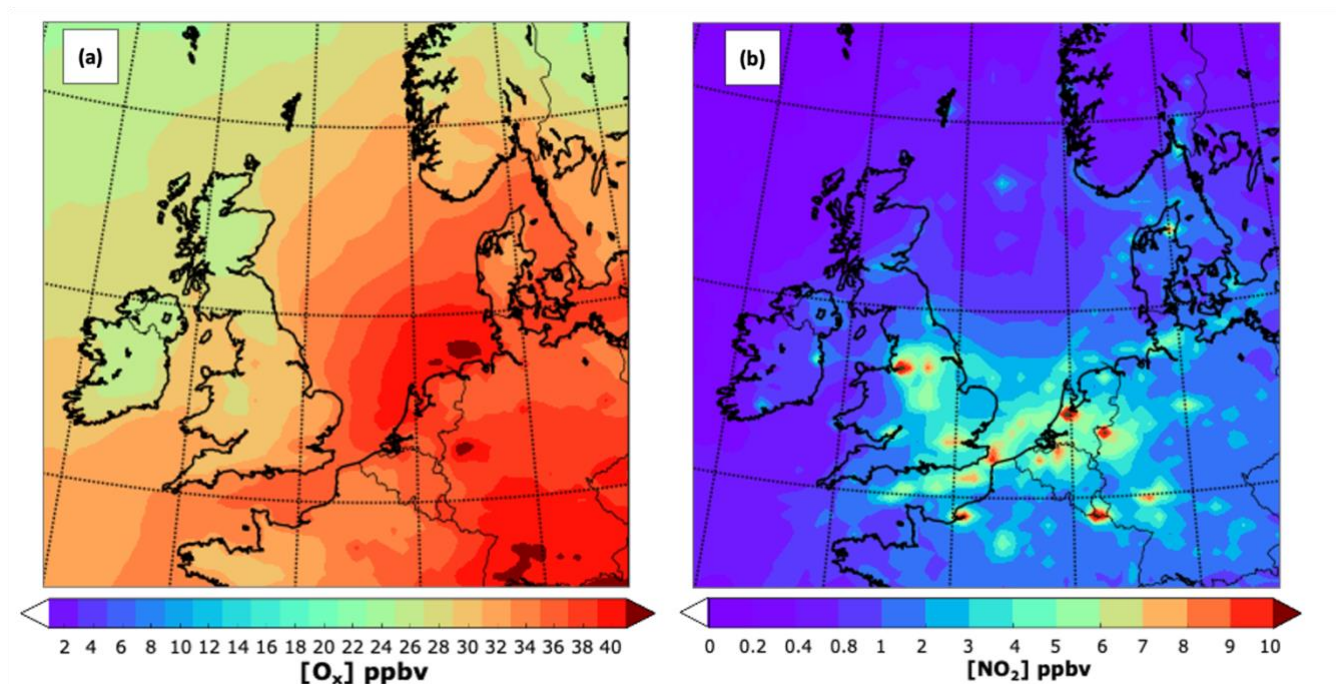
Figure 4. Close up of the spatial distribution for July 2015 of (a), mean O_x concentration (O_3 + NO_2) and (b) NO_2. Note the different scales.

645

650

655

660
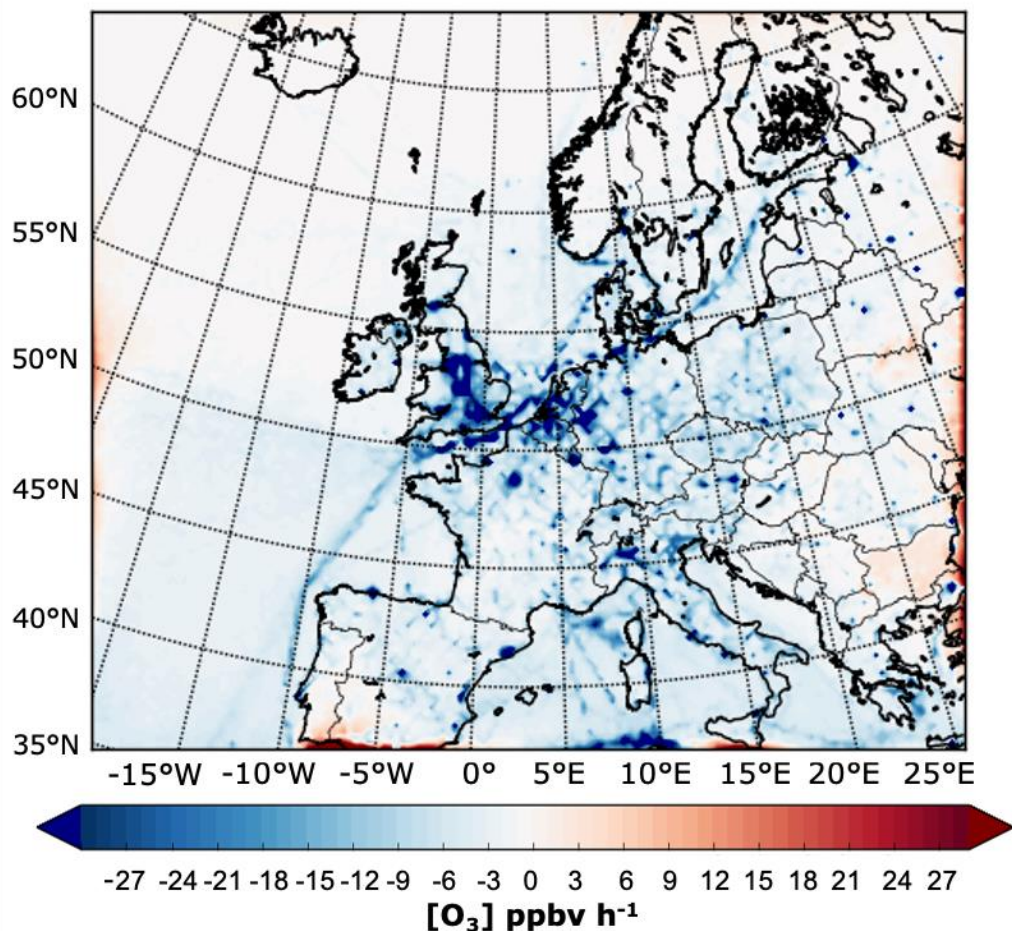
Figure 5. Net midday (11:00–14:00 UTC) near surface lateral boundary O_3 chemical production rate in ppbh^{-1} on July 2015. Note that O_3 production is driven by tagged LB NO_Y that has entered the model domain via the lateral boundaries.

665

670

675
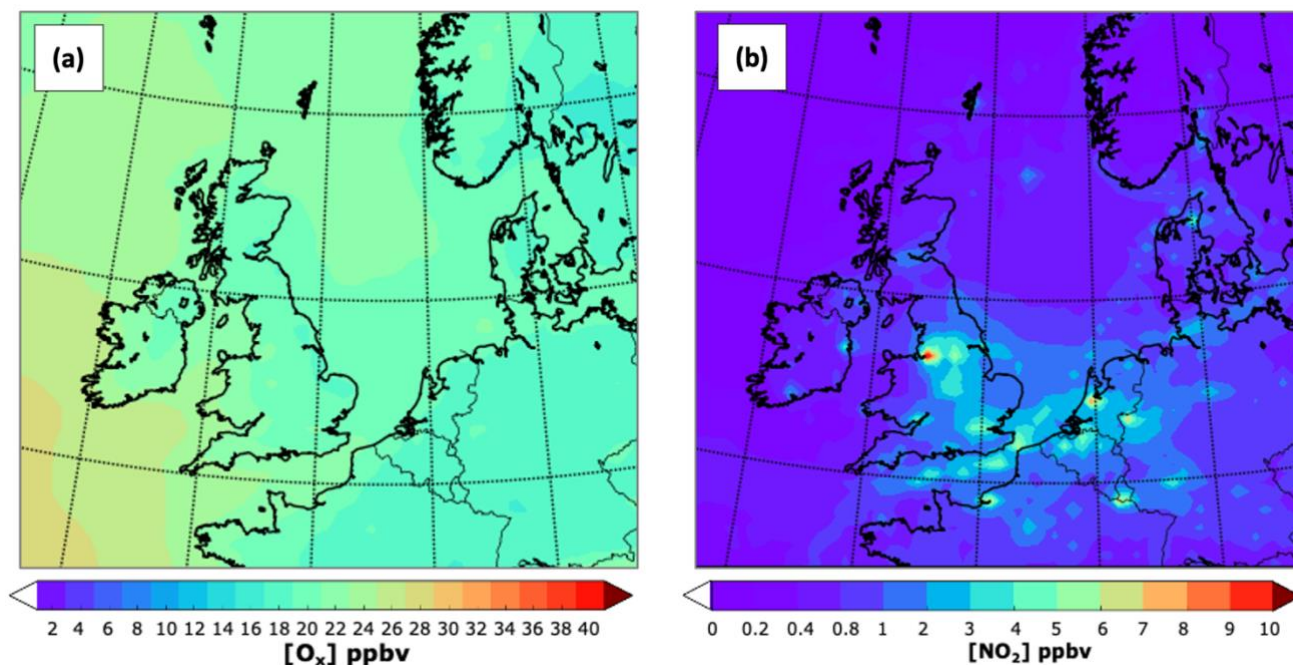
Figure 6. Closed up of the spatial distribution for July 2015 of (a) lateral boundary mean O_x concentrations ($O_3 + NO_2$), and (b) NO_2. Note the different scales in (b).

680

685

690

695

Atmospheric
Chemistry
and Physics
Discussions
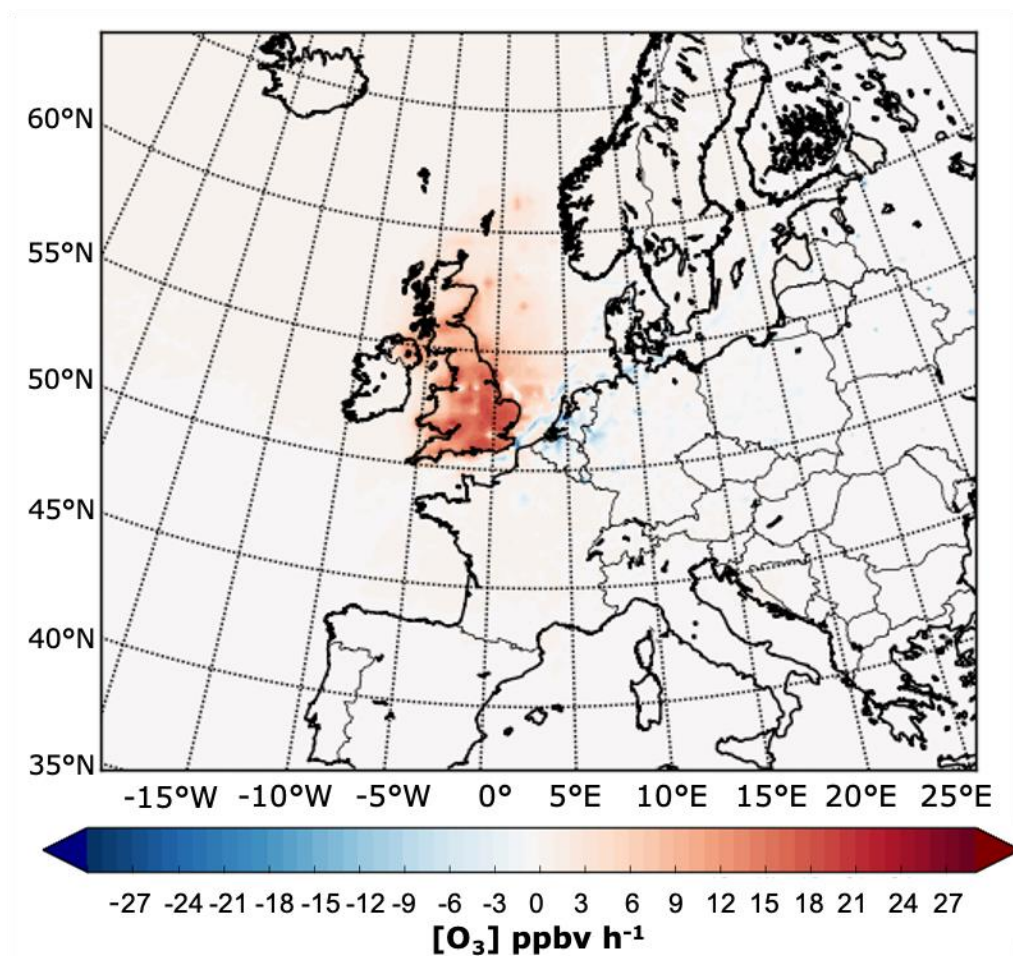
700 **Figure 7.** Net midday (11:00–14:00 UTC) surface chemical production rate in ppb h^{-1} for O_3 from UK anthropogenic NO_x emissions on July 2015.

705

710
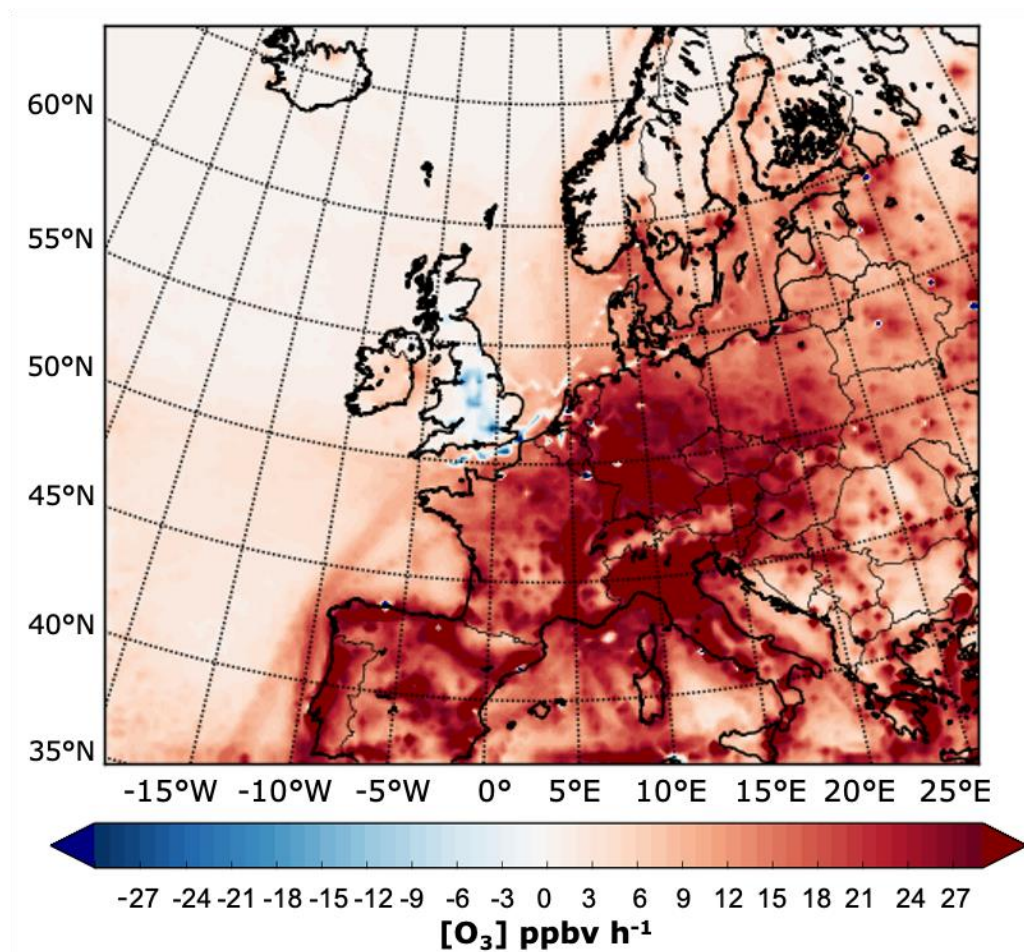
Figure 8. Net midday (11:00–14:00 UTC) surface chemical production rate in ppb h^{-1} for O$_3$ from European anthropogenic NO$_x$ emissions on July 2015.
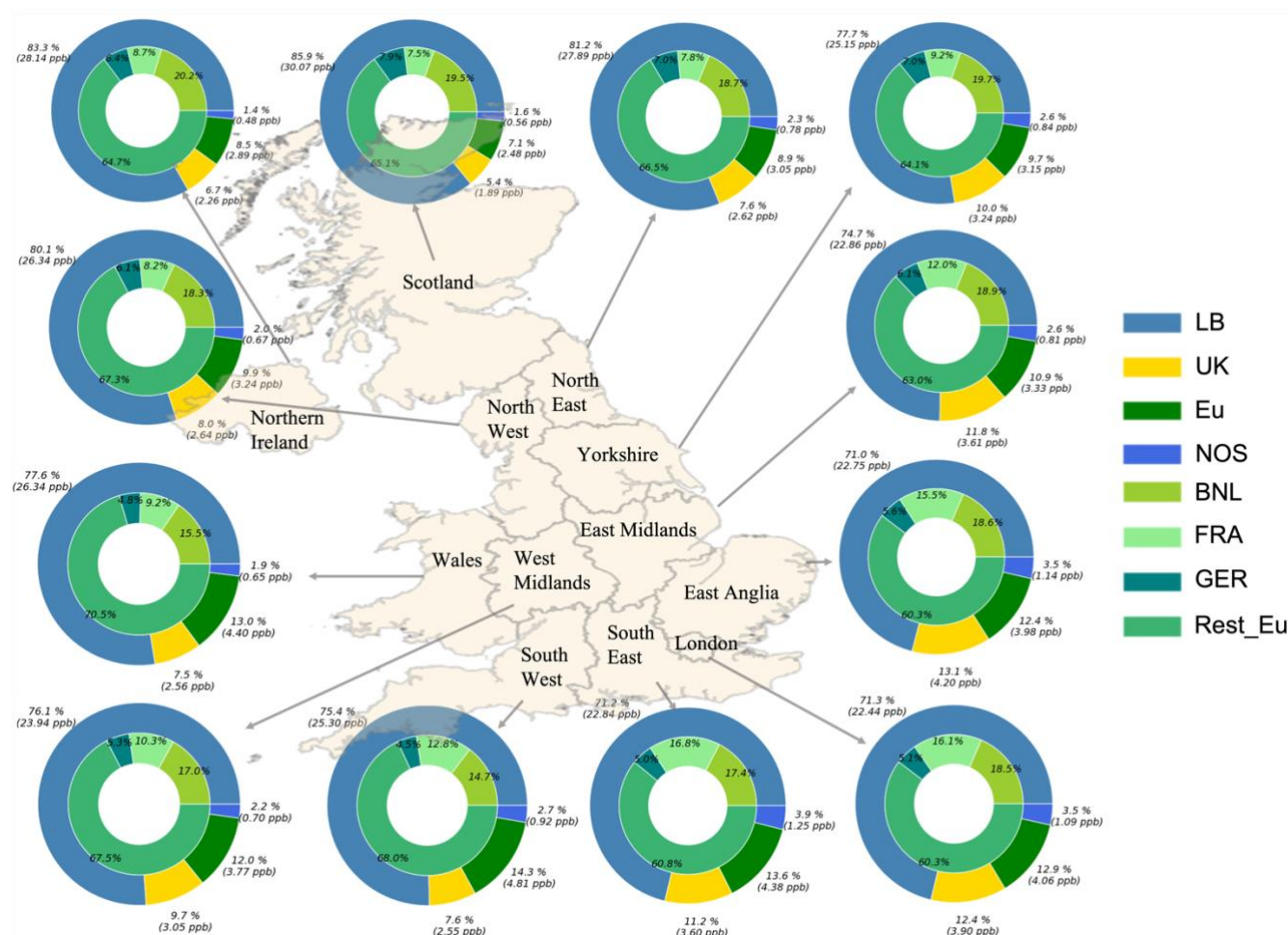
Figure 9. Simulated contributions to the mean O_3 mixing ratios in May 2015 over 12 receptors regions in the UK. Outer circle depicts the contributions from LB, UK, Eu super-region (Eu), and the NOS. The inner circle breaks down the contribution from the Eu super-region into four sub-regions: The Benelux (BNL), France (FRA), Germany (GER), and the rest of Europe (Rest_Eu). Note that the values correspond to the contributions from anthropogenic sources only, with the exception of the LB which includes O_3 from stratospheric origin.
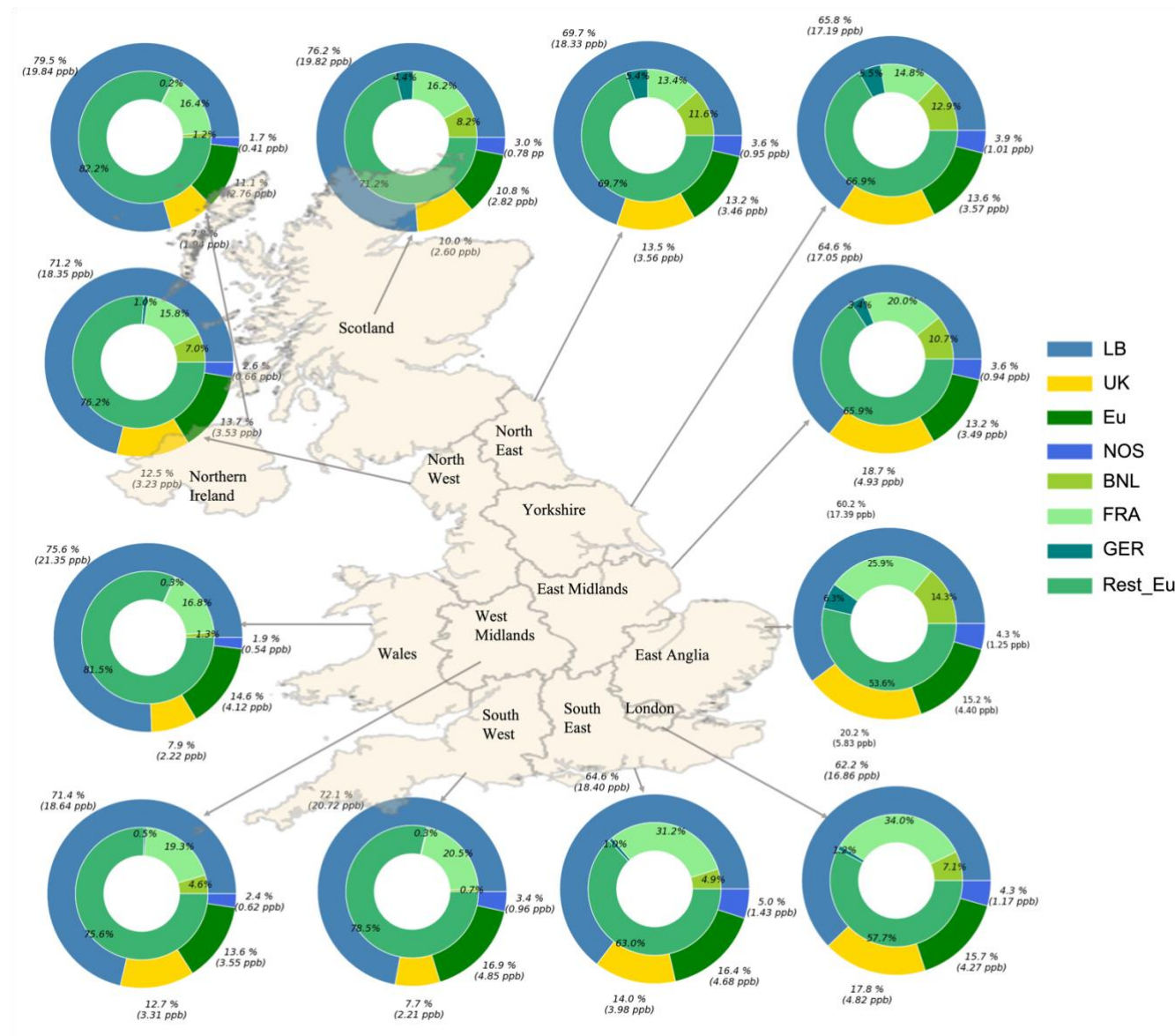
Figure 10. Simulated contributions to the mean O$_3$ mixing ratios in June 2015 over 12 receptors regions in the UK. Outer circle depicts the contributions from LB, UK, Eu super-region (Eu), and the NOS. The inner circle breaks down the contribution from the Eu super-region into four sub-regions: The Benelux (BNL), France (FRA), Germany (GER), and the rest of Europe (Rest_Eu). Note that the values correspond to the contributions from anthropogenic sources only, with the exception of the LB which includes O$_3$ from stratospheric origin.
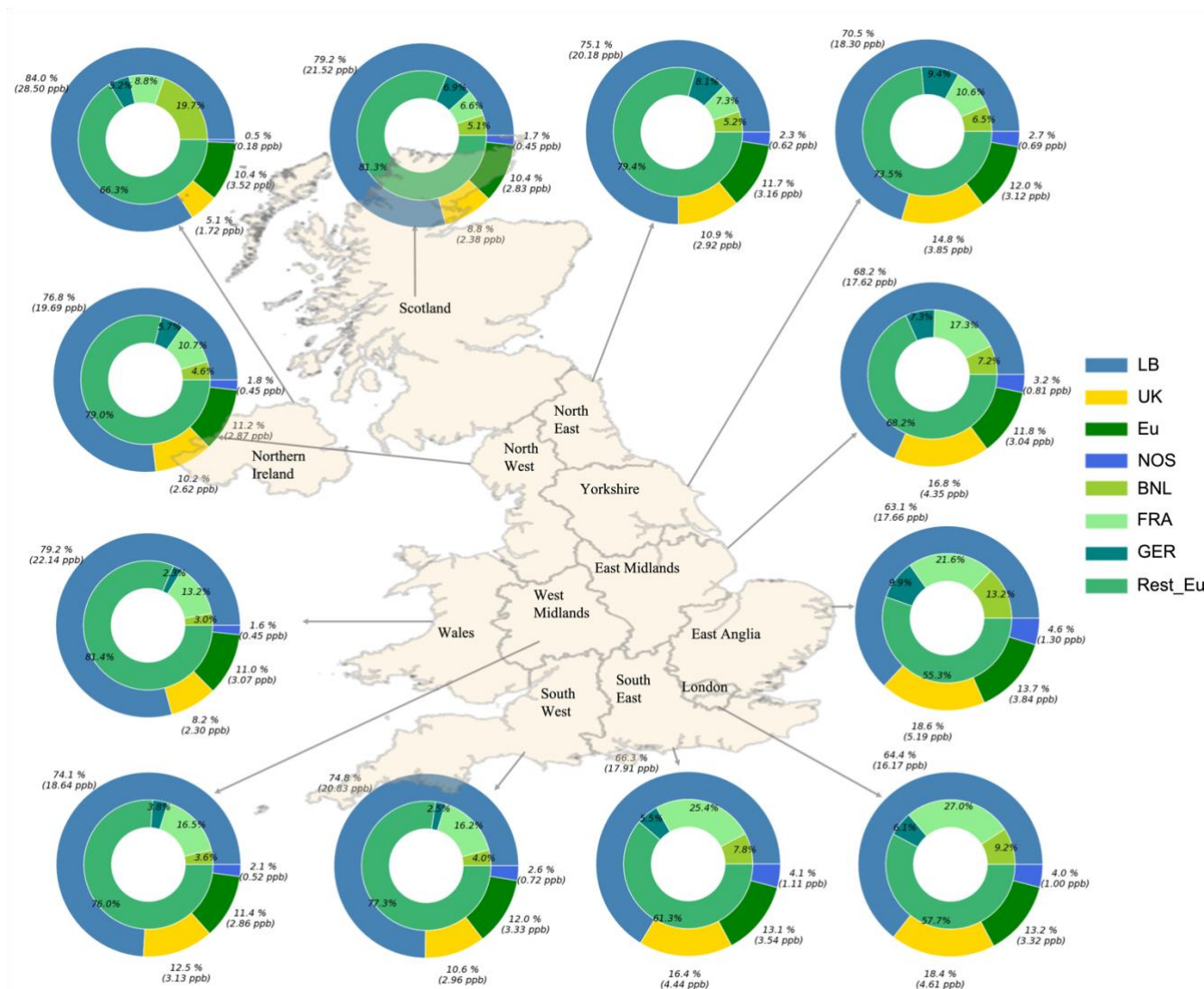
29

Atmospheric
Chemistry
and Physics
Discussions
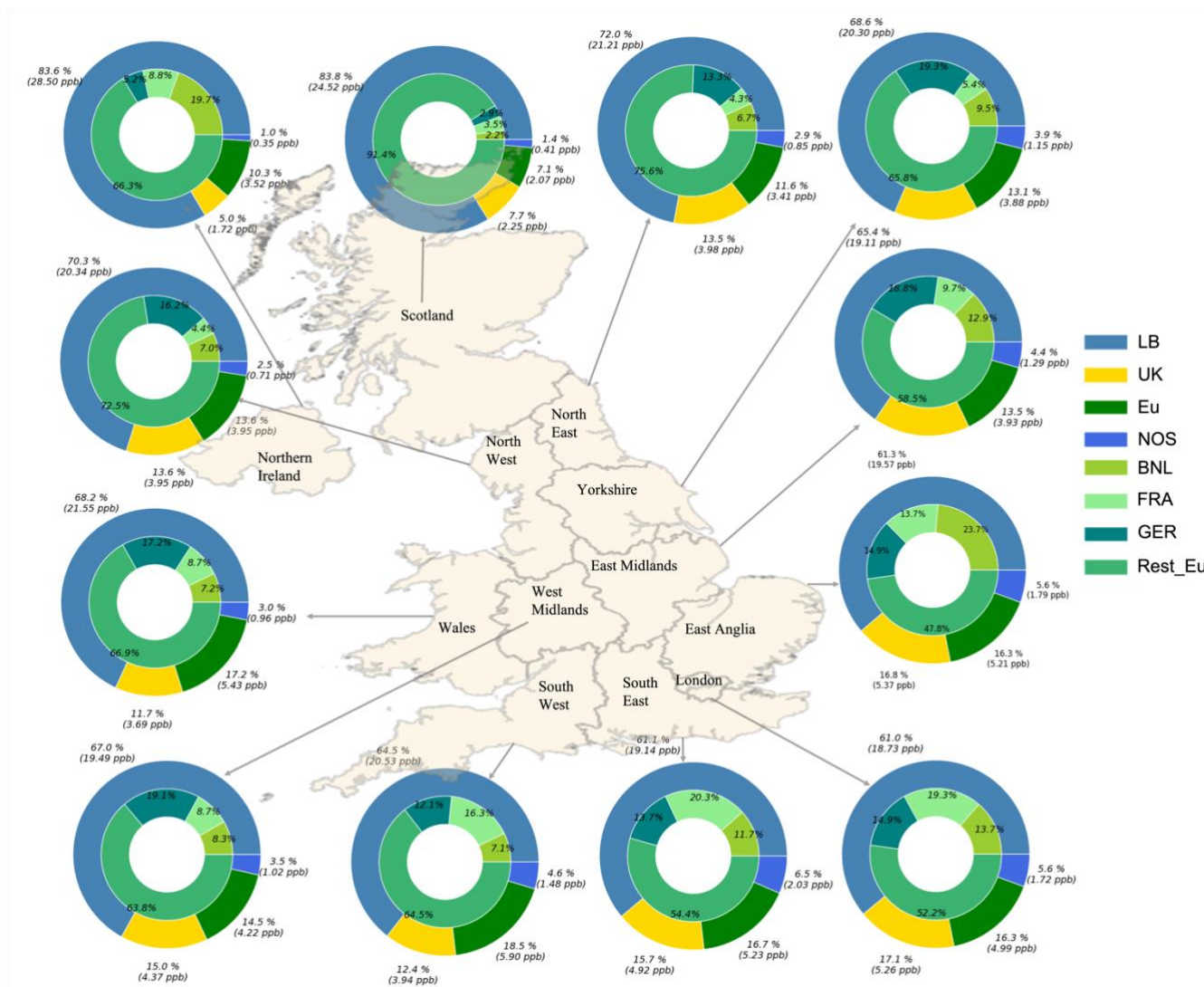
Figure 11. Simulated contributions to the mean O_3 mixing ratios in Julu 2015 over 12 receptors regions in the UK. Outer circle depicts the contributions from LB, UK, Eu super-region (Eu), and the NOS. The inner circle breaks down the contribution from the Eu super-region into four sub-regions: The Benelux (BNL), France (FRA), Germany (GER), and the rest of Europe (Rest_Eu). Note that the values correspond to the contributions from anthropogenic sources only, with the exception of the LB which includes O_3 from stratospheric origin.

Figure 12. Simulated contributions to the mean O$_3$ mixing ratios in August 2015 over 12 receptors regions in the UK. Outer circle depicts the contributions from LB, UK, Eu super-region (Eu), and the NOS. The inner circle breaks down the contribution from the Eu super-region into four sub-regions: The Benelux (BNL), France (FRA), Germany (GER), and the rest of Europe (Rest_Eu). Note that the values correspond to the contributions from anthropogenic sources only, with the exception of the LB which includes O$_3$ from stratospheric origin.
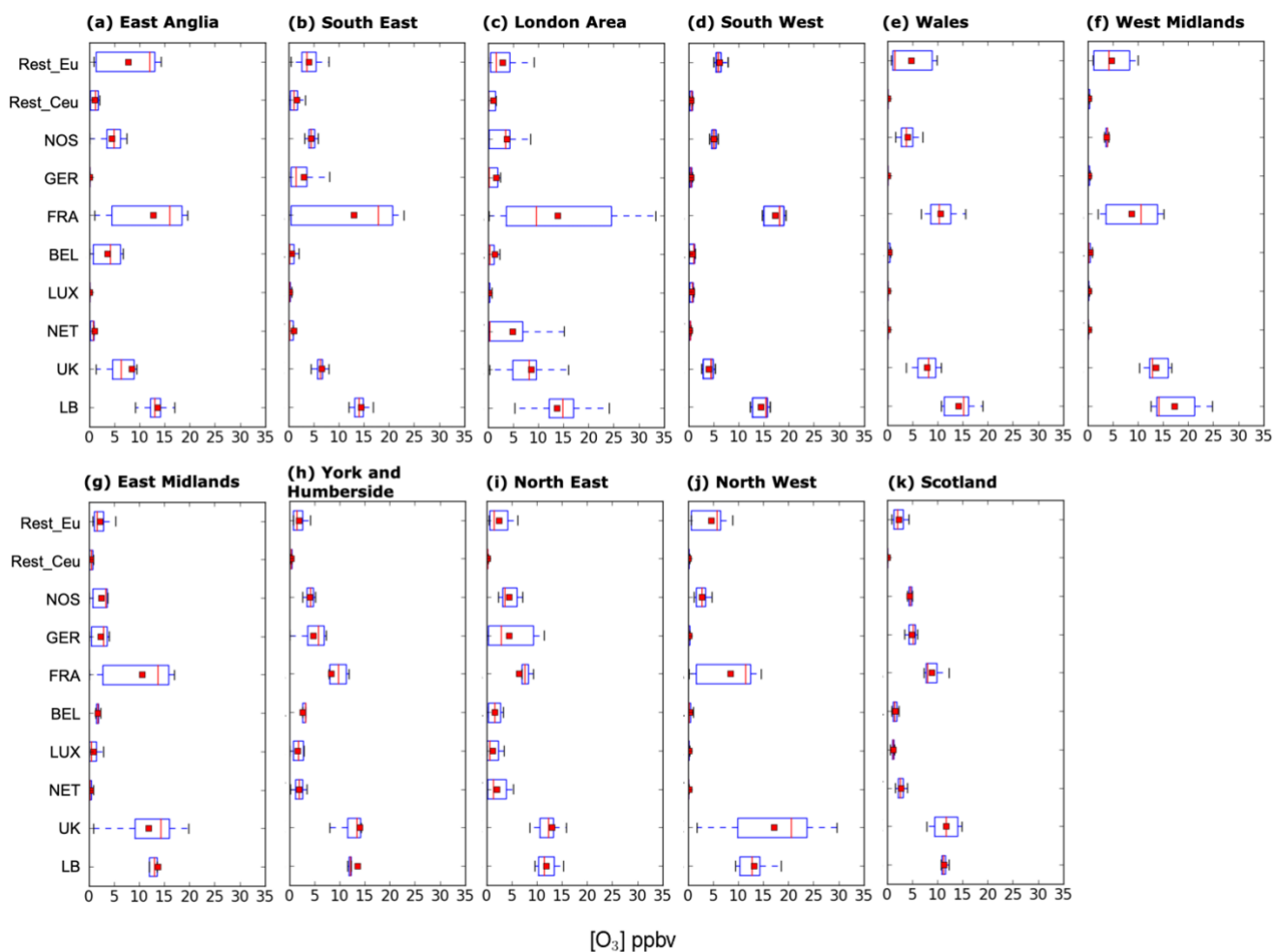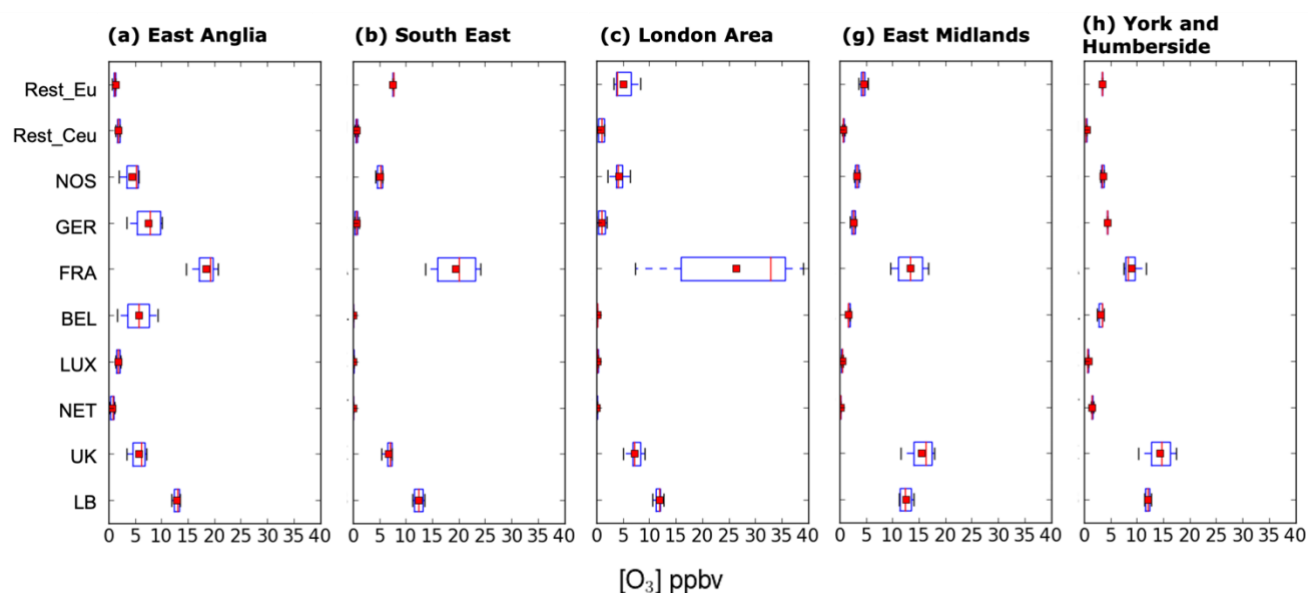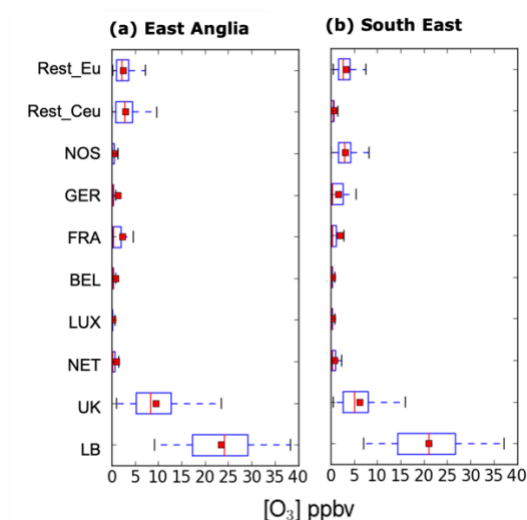
Figure 13. Hourly contributions, in ppbv, to surface O$_3$ at 11 UK receptor regions from 10 source regions (UK, background (LB), the Netherlands, Luxembourg, Belgium, France, Germany, rest of Central Europe (Rest_CEU), North Sea and English Channel (NOS) and rest of Eu) during days when the MDA8 is above 50 ppbv (number indicated in the header) between May and August. The lower and upper ends of the boxes indicate the 25th and 75th percentiles, the bars the medians, the dots the mean and the whiskers the minima and maxima.

815

Figure 14. Hourly contributions, in ppbv, to surface O_3 at 5 UK receptor regions from 10 source regions (UK, background (LB), the Netherlands, Luxembourg, Belgium, France, Germany, rest of Central Europe, North Sea and English Channel (NOS) and rest of Eu) during days when the MDA8 is above 60 ppbv (number indicated in the header) between May and August. The lower and upper ends of the boxes indicate the 25th and 75th percentiles, the bars the medians, the dots the mean and the whiskers the minima and maxima.

820

825

830

835

840

845

850 **Figure 15.** Hourly contributions, in ppbv, to surface O_3 at 2 UK receptor regions from 10 source regions (UK, background (LB), the Netherlands, Luxembourg, Belgium, France, Germany, rest of Central Europe, North Sea and English Channel (NOS) and rest of Eu) for AOT40 between May and August. The lower and upper ends of the boxes indicate the 25th and 75th percentiles, the bars the medians, the dots the mean and the whiskers the minima and maxima.

855